VOLUME ONE

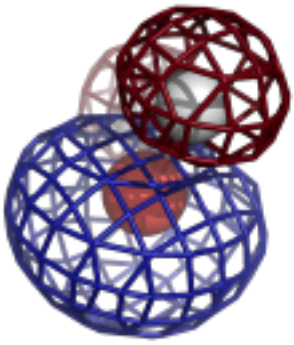

COMPUTATIONAL CRYSTALLOGRAPHY NEWSLETTER

JULY MMX

IOTBX.PDB SECONDARY-STRUCTURE SPOTFINDER

Table of Contents

Editor

Nigel W. Moriarty, NWMoriarty@LBL.Gov

Contributors

P. D. Adams, P. V. Afonine, V. B. Chen, N. Echols, J. J. Headd, R. W. Grosse-Kunstleve, N. W. Moriarty, D. C. Richardson, J. S. Richardson, N. K. Sauter, T. C. Terwilliger, A. Urzhumtsev

PHENIX News

New releases

A new feature in the *PHENIX* GUI is designed to compare the refined structures of similar proteins. Structure comparison uses the protein sequences to display the differences between each protein chain loaded in both a table format and graphically in *COOT*. Several features of the protein structure can be compared including rotamers and secondary structure. NCS chains can be overlaid in *COOT*, edited and saved in the original orientation.

The Java kinemage viewer *KiNG* (Protein Science 2009, 18:2403-2409) has been incorporated into *PHENIX*, so that the *KiNG* jar files and supporting scripts will be part of the distribution package, while relying on the Java virtual machine that is standard on the user's Mac or Linux platform. Without any other setup, the *KiNG* program in *PHENIX* would allow viewing of macromolecular structures directly from PDB files, and viewing of kinemages (such as multi-criterion kinemages from MolProbity). We are currently working to incorporate validation kinemage creation directly within the *PHENIX* GUI, allowing even more seamless and complete user evaluation of model quality during the refinement process. Later developments might also provide kinemage displays to provide help in evaluating other aspects of refinement and model building progress.

In a similar vein to `phenix.superpose_pdbs`, a new program has been added to *PHENIX* that is specifically designed for superposing ligands. Superposing protein models is generally done using the C_α positions. Ligands require different algorithms to create atomic correspondences, some of which has been implemented in *eLBOW*

The Computational Crystallography Newsletter (CCN) is a regularly distributed electronically via email and the PHENIX website, www.phenix-online.org/newsletter. Feature articles, meeting announcements and reports, information on research or other items of interest to computational crystallographers or crystallographic software users should be submitted to the editor at any time for consideration. Submission of text by email or word-processing files using the CCN templates is requested.

(Moriarty et. al., Acta Cryst., D65, 2009, 1074–1080). *eLBOW*'s methods including graph matching are used to match the atoms from a single molecule or group of residues to another single molecule. The resulting correspondences can be used in several ways. The molecules can be aligned using the least-squares residual of the distances between matched atoms; the exact position of the corresponding atoms can be transferred; or the PDB attributes such as atom name and residue name can be transferred. A file containing a protein and ligand can be used as input and multiple instances of the ligand can be handled. The program can be accessed by running `phenix.superpose_ligands`.

A tool developed especially for our industrial consortium members and designed to decrease the time to fit a ligand by using a previously positioned ligand in the same or similar protein model has been added to *PHENIX*. Guided Ligand Replacement (*GLR*) matches the protein models, determines the location of the fit ligand, performs an atomic match of the ligands and inserts the overlaid ligand into the apo protein model. As a final step, a real-space refinement is performed on the ligand and the surrounding protein. GLR attempts to match all instances of the guiding ligand in the asymmetric unit.

New features

RESOLVE in *PHENIX* is now entirely C++ code. This allows the use of the `cctbx` routines in *RESOLVE* and speeds up *RESOLVE* model-building by a factor of nearly two. It also allows caching of resolve libraries, further speeding up *RESOLVE* in *PHENIX*.

Ligand fitting in *PHENIX* now incorporates real-space refinement, yielding greatly improved fits of ligand to density.

Loop libraries have been created for rapid fitting of short loops with `phenix.fit_loops`.

The ligand geometry restraints editor, *REEL*, has a new feature that allows searching of the Chemical Components Dictionary available at http://www.wwpdb.org/ccd.html and also distributed with PHENIX. The user can search using various ligand attributes including name and chemical formula. The results can be viewed in the molecular viewing window.

Current PHENIX development

Work is currently underway to improve the support for carbohydrates in macromolecular models. The GlycoCT format (Herget et al., Carbohydr. Res., 2008, 343:2162-2171) which can specify a carbohydrate sequence has been chosen as the base format for file based input. Other formats will be supported. A GUI input is also being developed as well as tools to handle models already containing the carbohydrates. It is expected that ligand fitting will be expanded to improve the fitting of carbohydrates focusing on the saccharide chains that commonly occur in protein models. Branching will be supported from the inception.

Crystallographic meetings and workshops

2010 Australasian Crystallography School, 17-24 July, 2010

The 2010 Australasian Crystallography School is being held at the University of Queensland, Brisbane, Australia from the 17th to the 24th of July. Pavel Afonine will be teaching a module on macro-molecular refinement.

GRC – Diffraction Method in Crystallography, 18-23 July 2010

Several of the *PHENIX* developers will be attending the Gordon Conference entitled "Diffraction Methods in Crystallography" to be held at Bates College, Lewiston, Maine from the 18th to the 23rd of July. There will be posters on the various aspects of *PHENIX* including the graphical user interface, validation and ligands. Drop by during the poster sessions to speak to the developers.

ACA – 2010 Annual Meeting, 24-29 July, 2010

The annual meeting of the American Crystallographic Association will be held in Chicago, Illinois from the 24th to the 29th of July.

22nd PHENIX Workshop, 11-13 October, 2010

The semi-annual *PHENIX* workshop is being held in Cambridge, England from the 11th to the 13th of October. Developers will be presenting the latest programs and feature releases on Monday the

11th. All interested parties in the area are invited to attend the Monday sessions.

5th PHENIX User's Workshop, 14 October, 2010

Following the *PHENIX* Workshop in Cambridge U.K., a user's workshop will provide teaching and hands-on experience with *PHENIX* for the novice and expert.

Paris Workshop, 15 October, 2010

A contingent of *PHENIX* developers will be at Institut Pasteur, Paris, France on the 15th of October to participate in a workshop for the local users. The workshop is being organized by Claudine Mayer and Deshmukh Gopaul and is funded by the "Groupe Thematique Biologie" of the French Crystallography Association.

Expert advice

Geometry restraint ESD

Many users enquire about the details of the geometry restraints used in macromolecular refinement programs. Refmac, *COOT* and *PHENIX* use a CIF format; an example of the restraints for water appears at right.

```
data_comp_list
loop_
_chem_comp.id
_chem_comp.three_letter_code
_chem_comp.name
_chem_comp.group
_chem_comp.number_atoms_all
_chem_comp.number_atoms_nh
_chem_comp.desc_level
HOH         HOH 'water           ' ligand 3 1 .
data_comp_HOH
loop_
_chem_comp_atom.comp_id
_chem_comp_atom.atom_id
_chem_comp_atom.type_symbol
_chem_comp_atom.type_energy
_chem_comp_atom.partial_charge
_chem_comp_atom.x
_chem_comp_atom.y
_chem_comp_atom.z
HOH O  O OH2  .   -0.2400    0.0000   -0.3394
HOH H1 H HOH2 .    0.8400    0.0000   -0.3394
HOH H2 H HOH2 .   -0.6000    0.0000    0.6788
loop_
_chem_comp_bond.comp_id
_chem_comp_bond.atom_id_1
_chem_comp_bond.atom_id_2
_chem_comp_bond.type
_chem_comp_bond.value_dist
_chem_comp_bond.value_dist_esd
HOH  H1       O     single        1.080 0.020
HOH  H2       O     single        1.080 0.020
loop_
_chem_comp_angle.comp_id
_chem_comp_angle.atom_id_1
_chem_comp_angle.atom_id_2
_chem_comp_angle.atom_id_3
_chem_comp_angle.value_angle
_chem_comp_angle.value_angle_esd
HOH  H2       O      H1           109.47 3.000
```

Much of the information in the file is straightforward including atom names, elements and Cartesian coordinates. Even the bonding information is mostly transparent. The atoms involved, the type of bond and the ideal bond lengths are easily discerned. The last number on the line, however, is not so simple. The ESD is an Estimated Standard Deviation that allows a refinement program to estimate the gradients of the force on the two atoms in the bond using a parabola. The units of the ESD are the same as the ideal value so for bond lengths the unit is Ångstrom. The larger the ESD value, the more flexible the restraint will be in the refinement. Conversely, reducing the number will restrain the internal coordinate to remain closer to the ideal value.

There is a limit to the amount one can reduce the ESD of a restraint. In the extreme, setting the ESD value to zero will remove the restraint from the refinement. Also, reducing the ESD to a value that is orders of magnitude smaller than the other ESD values in the same class will greatly reduce the weight of the other restraints relative to the highly restrained value and may even adversely affect the weight of the x-ray term.

Generally, it is best to have the ESD values approximately the same as the expected accuracy of the experiment. In the case of the bond lengths, an ESD of 0.01 Ångstrom could be considered a reasonable lower bound. An angle ESD of about 1 degree and torsion ESD of 5 degrees are also reasonable as a lower limit.

FAQ

How do I create restraints for my ligand in PHENIX?

There are a number of ways. If you know the ligand code corresponding to the ligand in the PDB databases such as the Chemical Components, then you can use *eLBOW* thus:

```
phenix.elbow --chemical-component=ATP
```

The resulting files, `ATP.pdb` and `ATP.cif`, will have the data such as atom names consistent with the Chemical Components database.

cctbx PDB handling tools

Ralf W. Grosse-Kunstleve[a] and Paul D. Adams[a,b]

[a]*Lawrence Berkeley National Laboratory, Berkeley, CA 94720*
[b]*Department of Bioengineering, University of California at Berkeley, Berkeley, CA 94720*

Correspondence email: RWGrosse-Kunstleve@LBL.Gov

Introduction

The PDB format is the predominant working format for atomic parameters (coordinates, occupancies, displacement parameters, etc.) in macromolecular crystallography. Many small-molecule programs also support this format. The PDB format specifications are available at http://www.pdb.org/. Technically, the format is very simple, therefore a vast number of parsers exist in scientific packages. This article is about the PDB handling tools included in the Computational Crystallography Toolbox (`cctbx`, http://cctbx.sourceforge.net/), the open-source component of the *PHENIX* project (http://www.phenix-online.org/).

The evolution of the `cctbx` PDB handling tools has gone through three main stages spread out over several years. A simple parser implemented in Python has been available for a long time. In many cases Python's runtime performance is sufficient for interactive processing of PDB files, but can be limiting for large files, or for repeatedly traversing the entire PDB database. This has prompted us to implement a fast C++ parser that is described in Grosse-Kunstleve et al. (2006). However, initially the fast `cctbx` PDB handling tools only supported "read-only" access. Writing of PDB files was supported only at a very basic level. This shortcoming has been removed and the current cctbx version provides comprehensive tools for reading, manipulating, and writing PDB files. These tools are available from both Python and C++, under the `iotbx.pdb` module.

This article presents an overview of the main types in the `iotbx.pdb` module, considerations that lead to the design, and related important nomenclature. It is not a tutorial for using the `iotbx.pdb` facilities. For this, refer to http://cctbx.sourceforge.net/sbgrid2008/tutorial.html. See also http://cci.lbl.gov/hybrid_36/ which describes `iotbx.pdb` facilities for handling very large models.

Real-world PDB files

The simplicity of the PDB format is only superficial and, in the general case, stops after the initial parsing level. The structure of the PDB file implies a *hierarchy* of objects. A first approximation is this hierarchical view is:

```
model
  chain
    residue
      atom
```

This is only an approximation because of a feature that is easily overlooked at first: the "`altloc`" (official PDB nomenclature) column 17 of PDB ATOM records, specifying "alternative location" identifiers for atoms in alternative conformations. As it turned out, about 90% of the development time invested into `iotbx.pdb` was in some form related to alternative conformations. Our goal was to provide robust tools that work even for the most unusual (but valid) cases, since this is a vital characteristic of any automated system. The main difficulties encountered while pursuing this goal were:

- Chains with conformers that have different sequences
- Chains with duplicate `resseq+icode` (residue sequence number + insertion code)
- Conformers interleaved or separated

These difficulties are best illustrated with examples. An old version of PDB entry 2IZQ (from Aug 2008) includes a chain with conformers that have different sequences, the residue with `resseq` 11 in chain A, atoms 220 through 283:

```
HEADER    ANTIBIOTIC                              26-JUL-06   2IZQ
ATOM    220  N  ATRP A  11      20.498  12.832  34.558  0.50  6.03           N
................ATRP A  11 ..................................................
ATOM    243  HH2ATRP A  11      15.522   9.077  38.323  0.50 10.40           H
ATOM    244  N  CPHE A  11      20.226  13.044  34.556  0.15  6.35           N
................CPHE A  11 ..................................................
ATOM    254  CZ CPHE A  11      16.789   9.396  34.594  0.15 10.98           C
ATOM    255  N  BTYR A  11      20.553  12.751  34.549  0.35  5.21           N
................BTYR A  11 ..................................................
ATOM    261  CD1BTYR A  11      18.548  10.134  34.268  0.35  9.45           C
ATOM    262  HB2CPHE A  11      21.221  10.536  34.146  0.15  7.21           H
ATOM    263  CD2BTYR A  11      18.463  10.012  36.681  0.35  9.08           C
ATOM    264  HB3CPHE A  11      21.198  10.093  35.647  0.15  7.21           H
ATOM    265  CE1BTYR A  11      17.195   9.960  34.223  0.35 10.76           C
ATOM    266  HD1CPHE A  11      19.394   9.937  32.837  0.15 10.53           H
ATOM    267  CE2BTYR A  11      17.100   9.826  36.693  0.35 11.29           C
ATOM    268  HD2CPHE A  11      18.873  10.410  36.828  0.15  9.24           H
ATOM    269  CZ BTYR A  11      16.546   9.812  35.432  0.35 11.90           C
ATOM    270  HE1CPHE A  11      17.206   9.172  32.650  0.15 12.52           H
ATOM    271  OH BTYR A  11      15.178   9.650  35.313  0.35 19.29           O
ATOM    272  HE2CPHE A  11      16.661   9.708  36.588  0.15 11.13           H
ATOM    273  HZ CPHE A  11      15.908   9.110  34.509  0.15 13.18           H
ATOM    274  H  BTYR A  11      20.634  12.539  33.720  0.35  6.25           H
................BTYR A  11 ..................................................
ATOM    282  HH BTYR A  11      14.978   9.587  34.520  0.35 28.94           H
```

The original atom numbering does not have gaps. Here we have omitted blocks of atoms with constant `resname` and `resseq+icode` to save space.

As of Jun 8 2010, there are 74 files with mixed residue names in the PDB, i.e. only about 0.1% of the files. However, these files are perfectly valid and a PDB processing library is suitable as a component of an automated system only if it handles them sensibly.

An old version of PDB entry 1ZEH (Aug 2008) includes a chain with consecutive duplicate `resseq+icode`, atoms 878 through 894:

```
HEADER    HORMONE                                 01-MAY-98   1ZEH
HETATM  878  C1 ACRS     5      12.880  14.021   1.197  0.50 33.23           C
HETATM  879  C1 BCRS     5      12.880  14.007   1.210  0.50 34.27           C
................ACRS     5 ..................................................
HETATM  892  O1 ACRS     5      11.973  14.116   2.233  0.50 34.24           O
HETATM  893  O1 BCRS     5      11.973  14.107   2.248  0.50 35.28           O
HETATM  894  O   HOH      5      -0.924  19.122  -8.629  1.00 11.73           O
HETATM  895  O   HOH      6     -19.752  11.918   3.524  1.00 13.44           O
HETATM  896  O   HOH      7      -1.169  17.936  -6.103  1.00 12.89           O
```

To a human inspecting the old 1ZEH entry, it is of course immediately obvious that the water with `resseq` 5 is not related to the previous residue with `resseq` 5. However, arriving at this conclusion with an automatic procedure is not entirely straightforward. The human brings in the knowledge that water atoms without hydrogen are not covalently connected to other atoms. This is very detailed, specialized knowledge. Introducing such heuristics into an automatic procedure is likely to lead to surprises in some situations and is best avoided, if possible.

In the PDB archive, alternative conformers of a residue always appear consecutively. However, as mentioned in the introduction, the PDB format is also the predominant working format. Some programs produce files with conformers separated in this way (this file was provided to us by a user):

```
ATOM   1716  N  ALEU   190      28.628   4.549  20.230  0.70  3.78           N
ATOM   1717  CA ALEU   190      27.606   5.007  19.274  0.70  3.71           C
ATOM   1718  CB ALEU   190      26.715   3.852  18.800  0.70  4.15           C
ATOM   1719  CG ALEU   190      25.758   4.277  17.672  0.70  4.34           C
ATOM   1829  N  BLEU   190      28.428   4.746  20.343  0.30  5.13           N
ATOM   1830  CA BLEU   190      27.378   5.229  19.418  0.30  4.89           C
ATOM   1831  CB BLEU   190      26.539   4.062  18.892  0.30  4.88           C
ATOM   1832  CG BLEU   190      25.427   4.359  17.878  0.30  5.95           C
ATOM   1724  N  ATHR   191      27.350   7.274  20.124  0.70  3.35           N
ATOM   1725  CA ATHR   191      26.814   8.243  21.048  0.70  3.27           C
ATOM   1726  CB ATHR   191      27.925   9.229  21.468  0.70  3.73           C
ATOM   1727  OG1ATHR   191      28.519   9.718  20.259  0.70  5.22           O
ATOM   1728  CG2ATHR   191      28.924   8.567  22.345  0.70  4.21           C
ATOM   1729  C  ATHR   191      25.587   8.983  20.559  0.70  3.53           C
ATOM   1730  O  ATHR   191      24.872   9.566  21.383  0.70  3.93           O
                        ... residues 191 through 203 not shown
ATOM   1828  O  AGLY   203       8.948  14.861  23.401  0.70  5.84           O
ATOM   1833  CD1BLEU   190      26.014   4.711  16.521  0.30  6.21           C
ATOM   1835  C  BLEU   190      26.506   6.219  20.135  0.30  4.99           C
ATOM   1836  O  BLEU   190      25.418   5.939  20.669  0.30  5.91           O
ATOM   1721  CD2ALEU   190      24.674   3.225  17.536  0.70  5.31           C
ATOM   1722  C  ALEU   190      26.781   6.055  20.023  0.70  3.36           C
ATOM   1723  O  ALEU   190      25.693   5.796  20.563  0.70  3.68           O
ATOM   8722  C  DLEU   190      26.781   6.055  20.023  0.70  3.36           C
ATOM   8723  O  DLEU   190      25.693   5.796  20.563  0.70  3.68           O
ATOM   9722  C  CLEU   190      26.781   6.055  20.023  0.70  3.36           C
ATOM   9723  O  CLEU   190      25.693   5.796  20.563  0.70  3.68           O
```

In this file, conformers A and B of residue 190 appear consecutively, but conformers C and D appear only after conformers A and B of all residues 191 through 203. While this is not the most intuitive way of ordering the residues in a file, it is still considered valid because the original intention is clear. Since it was our goal to develop a comprehensive library suitable for automatically processing files produced by any popular program, we found it important to correctly handle non-consecutive conformers.

iotbx.pdb.hierarchy

When developing the procedure capable of handling the variety of real-world situations shown above, we strived to keep the underlying rule-set as simple as possible and to avoid highly specific heuristics (e.g. "water is never covalently bound"). Complex rules imply complex implementations, are difficult to explain and understand, tend to lead to surprises, and are therefore likely to be rejected by the community. With this and the real-world situations in mind, we arrived at the following *primary* organization of the PDB hierarchy:

```
Primary PDB hierarchy:

  model(s)
    id
    chain(s)
      id
      residue_group(s)
        resseq
        icode
        atom_group(s)
          resname
          altloc
          atom(s)
```

In this presentation the "(s)" indicates a list of objects of the given type. i.e. a hierarchy contains a list of models, each model has an "`id`" (a simple string) and holds a list of chains, etc.

Comparing with the "first approximation hierarchy" above, the `residue` type is replaced with two new types: `residue_group` and `atom_group`. These types had to be introduced to cover all the real-world cases shown above. The `residue_group` and `atom_group` types are new and unusual. Before we go into the details of these types, it will be helpful to consider the bigger picture by introducing the alternative *secondary* view of the PDB hierarchy:

```
Secondary view of PDB hierarchy:

  model(s)
    id
    chain(s)
      id
      conformer(s)
        altloc
        residue(s)
          resname
          resseq
          icode
          atom(s)
```

This organization is probably more intuitive at first. The first two levels (`model`, `chain`) are exactly the same as in the primary hierarchy. Each chain holds a list of `conformer` objects, which are characterized by the `altloc` character from column 17 in the PDB ATOM records. A `conformer` is understood to be a *complete copy* of a chain, but usually two conformers *share* some or even most atoms. A `residue` is characterized by a unique `resname` and the `resseq+icode`.

The secondary view of the hierarchy evolved in the context of generating geometry restraints for refinement (e.g. bond, angle, and dihedral restraints), where this organization is most useful. It is also the organization introduced in Grosse-Kunstleve et al. (2006), where it was actually the primary organization. While working with the conformer-residue organization, we found that it is difficult to manipulate a hierarchy (e.g. add or delete atoms) in obvious ways. Finally, while developing the automatic generation of constrained occupancy groups for alternative conformations, the conformer-residue organization proved to be unworkable. The main difficulty is that the relative order of residues with alternative conformations is lost in the conformer-residue organization; it is only given indirectly by interleaved residues with shared atoms -- if they exist. As convenient as the `conformer-residue` organization is for the generation of restraints, it is a hindrance for other purposes.

The names for the new types in the primary hierarchy were chosen not to collide with the secondary view. We could have used "`conformer`" and "`residue`" again, just reversed, but there would be the big surprise that one residue has different `resnames`. To send the signal "this is not what you usually think of as a residue", we decided to use `residue_group` as the type name. A residue group holds a list of `atom_group` objects. All atoms in an atom group have the same `resname` and `altloc`. Therefore "`resname_altloc_group`" would have been another plausible name, but we favored `atom_group` since it is more concise and better conveys what is the main content.

Detection of residue groups and atom groups

When constructing the primary hierarchy given a PDB file, the processing algorithm has to detect models, chains, residue groups, atom groups and atoms. Most steps are fairly straightforward, but none of the steps is actually completely trivial. For example, what to do if TER or ENDMDL cards are missing? What if residue sequence numbers are not consecutive? The ribosome community widely uses `segid` instead of chain `id` (even though the `segid` column is officially deprecated by the PDB). What if a file

contains both chain `id` and `segid`? Documenting all our answers in full detail is beyond the scope of this article (and would be more distracting than helpful anyway because the source code is openly available). Therefore we concentrate on the most important rules for the detection of residue groups and atom groups.

Then central conflict we had to resolve was:

- In order to handle non-consecutive conformers, we have to use the `resseq+icode` to find and group related residues.
- However, we cannot use the `resseq+icode` alone as a guide, because we also want to handle chains with duplicate `resseq+icode` (consecutive or non-consecutive).

This lead to a two stage procedure. In the first stage:

- A residue group is given by a block of consecutive ATOM or HETATM records with identical `resseq+icode` columns (SIGATM, ANISOU, and SIGUIJ records may be interleaved), e.g.

```
ATOM    234  H   ATRP A  11      20.540  12.567  33.741  0.50  7.24           H
ATOM    235  HA ATRP A  11      20.771  12.306  36.485  0.50  6.28           H
ATOM    244  N   CPHE A  11      20.226  13.044  34.556  0.15  6.35           N
ATOM    245  CA CPHE A  11      20.950  12.135  35.430  0.15  5.92           C
```

However, there is an important pre-condition:

- Unless a sub-block of ATOM records with identical `resname+resseq+icode` columns contains a main-conformer atom (almost "blank `altloc`"), e.g.

```
HEADER    ANTIBIOTIC RESISTANCE                   07-MAY-97   1AJQ
CRYST1   52.120   65.080   76.300 100.20 111.44 105.81 P 1           1
HETATM 6097 CA    CA     1       5.676  34.115  52.446  1.00 18.50          CA
HETATM 6100  C2  SPA     1      11.860  36.159  33.853  1.00 14.30           C
HETATM 6107  C6  SPA     1      13.085  36.522  34.644  1.00 17.34           C
```

In this case the sub-block is assigned to a separate residue group.

Within each residue group, all atoms are grouped by `altloc+resname` and assigned to atom groups. The order of the atoms in a residue group does not affect the assignment to atom groups.

After all atom records are assigned to residue groups and atom groups,

- residue groups with identical `resseq+icode`
- that do not contain main-conformer atoms

are merged in the second processing stage. While two residue groups are merged, atom groups with identical `altloc+resname` from the two sources are also merged.

Note that the grouping steps in this process may change the order of the atoms. However, our implementation preserves the relative order of the atoms as much as possible. I.e. in the hierarchy, `resseq+icode` appear in the original "first seen" order, and similarly for `altloc+resname` within a residue group.

Construction of secondary view of hierarchy

The secondary view of the hierarchy is constructed trivially from the primary hierarchy objects. For each chain, the complete list of `altloc` characters is determined in a first pass. In a second pass, a conformer object is created for each `altloc`, and a second loop over the chain assigns the atoms to each conformer. Main-conformer atoms are assigned to all conformers, atoms in alternative

conformations only to the corresponding conformer. Because of the difficulties alluded to earlier, the conformer and residue objects in the secondary view are "read-only". I.e. all manipulations such as addition or removal of residues, have to be performed on the primary hierarchy. Re-constructing the secondary view after the primary hierarchy has been changed is very fast (fractions of seconds even for the largest files, e.g. 0.22 s for PDB entry 1HTQ with almost one million atoms).

The `iotbx/examples/pdb_hierarchy.py` script shows how to construct the primary hierarchy from a PDB file, and how to obtain the secondary view.

Nomenclature related to alternative conformations

The `iotbx.pdb` module uses the following nomenclature to describe various aspects of alternative conformations:

- ***Main conf. atom*** : an atom with
  - a blank `altloc` character
  - and no other atom with the same `name+resname` (but different `altloc`) in the residue group. This second condition is needed for cases like this:

```
HEADER    HYDROLASE                               12-MAR-04   1SO7
ATOM   2460  CG1 VAL A 325     -23.284  97.713  15.815  0.66 21.74           C
ATOM   2461  CG1AVAL A 325     -23.010  97.616  18.295  0.66 22.88           C
ATOM   2462  CG2BVAL A 325     -24.819  96.373  17.146  0.66 22.57           C
```

- ***Alt. conf. atom*** : not main conf.
- ***Conformer*** : a complete chain with main conf. atoms and alt. conf. atoms with a specific `altloc`.

  Note for completeness: it is also possible to obtain conformers of an individual residue group. However, conceptually this is best viewed as a shortcut for first obtaining the conformers of a chain, and then finding the residue of interest in each conformer, ignoring all other residues.

- ***Residue*** : complete residue in a conformer with main conf. atoms and alt. conf. atoms.

Residues are classified as follows:

- ***pure main conf.*** : all main conf. atoms
- ***pure alt. conf.*** : all alt. conf. atoms
- ***proper alt. conf.*** : both main conf. atoms and alt. conf atoms, all alt conf. atoms have a non-blank `altloc` column
- ***improper alt. conf.*** : both main conf. atoms and alt. conf atoms, one or more alt conf. atoms have a blank `altloc` column (as shown in the 1SO7 fragment above).

Errors and warnings

The tools in `iotbx.pdb` are designed to be as tolerant as reasonably possible when processing input PDB files. E.g., as of Jun 8 2010, all 65802 files in the PDB archive can be processed without generating exceptions. However, to assist users and developers in creating PDB files without ambiguities, the hierarchy object provides methods for flagging likely problems as errors and warnings. It is up to the application how to react to the diagnostics.

The `phenix.pdb.hierarchy` command can be used to quickly obtain a summary of the hierarchy in a PDB file and some diagnostics. This example command highlights all main features:

```
phenix.pdb.hierarchy pdb1jxw.ent.gz
```

Output:

```
file pdb1jxw.ent.gz
  total number of:
    models:       1
    chains:       2
    alt. conf.:   5
    residues:    49
    atoms:      786
    anisou:       0
  number of atom element+charge types: 5
  histogram of atom element+charge frequency:
    " H  " 383
    " C  " 261
    " O  "  77
    " N  "  59
    " S  "   6
  residue name classes:
    "common_amino_acid" 48
    "other"              1
  number of chain ids: 2
  histogram of chain id frequency:
    " " 1
    "A" 1
  number of alt. conf. ids: 3
  histogram of alt. conf. id frequency:
    "A" 2
    "B" 2
    "C" 1
  residue alt. conf. situations:
    pure main conf.:     32
    pure alt. conf.:      3
    proper alt. conf.:   14
    improper alt. conf.:  0
  chains with mix of proper and improper alt. conf.: 0
  number of residue names: 16
  histogram of residue name frequency:
    "CYS" 6
    "THR" 6
    "ALA" 5
    "ILE" 5
    "PRO" 5
    "GLY" 4
    "ASN" 3
    "SER" 3
    "ARG" 2
    "LEU" 2
    "TYR" 2
    "VAL" 2
    "ASP" 1
    "EOH" 1    other
    "GLU" 1
    "PHE" 1
  ### WARNING: consecutive residue_groups with same resid ###
  number of consecutive residue groups with same resid: 2
    residue group:
      "ATOM    378  N   PRO A  22 .*.     N  "
      ... 12 atoms not shown
      "ATOM    391  HD3APRO A  22 .*.     H  "
    next residue group:
      "ATOM    392  CB BSER A  22 .*.     C  "
      ... 6 atoms not shown
      "ATOM    399  HB3CSER A  22 .*.     H  "
    ----------------------------------------
    residue group:
      "ATOM    432  N   LEU A  25 .*.     N  "
      ... 18 atoms not shown
      "ATOM    439  CD1CLEU A  25 .*.     C  "
    next residue group:
      "ATOM    452  CG1BILE A  25 .*.     C  "
      ... 13 atoms not shown
      "ATOM    466 HD13CILE A  25 .*.     H  "
```

The diagnostics are mainly intended for PDB working files, but we have tested the `iotbx.pdb` module by processing the entire PDB archive. (This took about 3700 CPU seconds, but using 40 CPUs the last job finished after only 277 seconds. Disk and network I/O is rate-limiting in this case, not the performance of the PDB handling library.) The results are summarized in the following table:

```
Total number of .ent files: 65802 (2010 Jun 8)

56873   WARNING: duplicate chain id
    3   WARNING: consecutive residue_groups with same resid
    2   ERROR:   duplicate atom labels
    1   ERROR:   improper alt. conf.
    0   ERROR:   duplicate model id
    0   ERROR:   residue group with multiple resnames using same altloc
```

About 86% of the PDB entries re-use the same chain id for multiple chains (which are either separated by other chains or TER cards). In many cases, the re-used chain id is the blank character, which is clearly a minor issue. However, we flag this situation to assist people in producing new PDB files with unambiguous chain ids.

The next item in the list, "consecutive residue_groups with same resid" (where `resid=resseq+icode`), was mentioned before. This situation is best avoided to minimize the chances of mis-interpreting the PDB files.

"duplicate atom labels" pose a serious practical problem (therefore flagged as "ERROR") since it is impossible to uniquely select atoms with duplicate labels, for example via an atom selection syntax as used in many programs (*CNS*, *PyMOL*, *PHENIX*, *VMD*, etc.) or via PDB records in the connectivity annotation section (LINK, SSBOND, CISPEP). Atom serial numbers are not suitable for this purpose since many programs do not preserve them.

Only one PDB entry (1JRT) includes "improper alt. conf." as introduced in the previous section.

There are no PDB entries with two other potential problems diagnosed by the iotbx.pdb module. MODEL ids are unique throughout the PDB archive (as an aside: and all MODEL records have a matching ENDMDL record). Finally, in all 74 files with mixed residue names (i.e. conformers with different sequences), there is exactly one residue name for a given altloc.

Acknowledgments

We gratefully acknowledge the financial support of NIH/NIGMS under grant number P01GM063210. Our work was supported in part by the US Department of Energy under Contract No. DE-AC02-05CH11231.

References

Grosse-Kunstleve, R.W., Zwart, P.H., Afonine, P.V., Ioerger, T.R., Adams, P.D. (2006). Newsletter of the IUCr Commission on Crystallographic Computing, 7, 92-105.

Secondary structure restraints in phenix.refine

Nathaniel Echols[a], Jeffrey J. Headd[a], Pavel Afonine[a], and Paul D. Adams[a,b]

[a]*Lawrence Berkeley National Laboratory, Berkeley, CA 94720*

[b]*Department of Bioengineering, University of California at Berkeley, Berkeley, CA 94720*

Correspondence email: NEchols@LBL.Gov

Introduction

We have implemented simple, automatic restraints for common secondary structure elements in proteins and nucleic acids, which can help reduce over-fitting at low-to-moderate resolution and preserve the secondary structure geometry that can be distorted due to the low resolution. Internally, these are simply distance restraints between hydrogen-bonding atoms in helices, sheets, or nucleic acid base pairs, with or without explicit hydrogens. The current method has the advantage of being fast, easily reduced to relatively simple input parameters, and useful for improving poor-quality regions of structure where the bonding may not be automatically recognized.

General description and syntax

A new command for identifying secondary structure and generating the necessary parameters, `phenix.secondary_structure_restraints`, was introduced in version 1.6.1, and most of the functionality is also accessible through `phenix.refine` itself. In the absence of user-defined atom selections, or if the parameter `find_automatically=True` is set, the program will look first in the header of the input PDB file(s) and parse any HELIX and SHEET records (*Figure 1*). Note that when

```
HELIX    8   8 ASP A  181  ARG A  191  1                                  11
HELIX    9   9 SER A  192  ASP A  194  5                                   3
HELIX   10  10 SER A  195  GLN A  209  1                                  15
SHEET    1   A 5 ARG A  13   ASP A  14   0
SHEET    2   A 5 LEU A  27   SER A  30  -1  O  ARG A  29   N  ARG A  13
SHEET    3   A 5 VAL A 156  HIS A 159   1  O  VAL A 156  N  PHE A  28
SHEET    4   A 5 ASP A  51   ASP A  54   1  N  ALA A  51   O  LEU A 157
SHEET    5   A 5 ASP A  74   LEU A  77   1  O  HIS A  74   N  VAL A  52
```

Figure 1. Beta PDB syntax for secondary structure records (excerpted from PDB ID 1ywf; Grundner et al. 2005).

running from `phenix.refine`, a different scope requires the use `secondary_structure.input.find_automatically=True`. If none are found, the open-source program *KSDSSP* (UCSF Computer Graphics Laboratory; Kabsch & Sander 1983) is used to generate these records based on the input geometry. Because the PDB format uses fixed columns (Bernstein et al. 1977, Berman et al. 2000) and is not easily edited, the records are converted to an intermediate format using the same parameter syntax and atom selection language as other programs in *PHENIX* (*Figure 2*; Adams et al. 2010). Example of use:

```
phenix.secondary_structure_restraints model.pdb > ss.eff
```

Although the PDB format specification provides for ten types of alpha helix, only the three most commonly found in natural proteins are processed: alpha (forming bonds between the carbonyl oxygen of residue n and the amide nitrogen of residue n+4), 3_{10} (n+3), and pi (n+5). As the alpha form is by far the most common, this is the default helix type. Beta strands have only two types, parallel and antiparallel, which can coexist in a single sheet (*Figure 3*). The parameter blocks for sheets are considerably more complicated because of the order-dependency of individual strands, and the requirement of explicit annotation of the start and end of hydrogen bonding between strand pairs. The parameters may be freely edited to add or remove secondary structure groups, but we recommend minimal changes to the sheets, due to the complexity of the definitions.

From within `phenix.refine` (Afonine et al. 2005), use of the restraints may be activated with the parameter `main.secondary_structure_restraints=True`. If no helix or sheet atom selections are included in the input parameters, the automatic identification procedure will be run; otherwise, the existing parameters are used without modification. Once secondary structure is assigned it is maintained for the rest of the refinement, but future versions will probably add the option to re-annotate the structure after each macro-cycle. The log file (and console output) will contain information about the overall secondary structure content, if any.

Hydrogen bond parameterization

Hydrogen bonds are modeled as simple harmonic restraints; we have not attempted to use a more physically rigorous hydrogen-bonding potential (for example, Fabiola et al. 2002). For maximum flexibility, either explicit or implicit hydrogen bonds are supported; the latter use a longer distance restraint between heavy atoms. The methods for converting atom selections into hydrogen bonds relies on several assumptions:

- The order of residues in the input PDB file exactly corresponds to the order in the protein itself
- Each secondary structure element is continuous with no missing residues
- All residues are complete, with no missing atoms

Unless the PDB file has undergone significant manual editing, these conditions are unlikely to be violated. The main exception is in the handling of hydrogen atoms, which are handled inconsistently by different crystallography applications. The program will first examine the PDB file to determine whether hydrogens are present, in which case it defaults to explicit hydrogen bonds. However, if newly built residues are missing hydrogen atoms, they will not be properly restrained. This can be remedied by running

```
refinement.secondary_structure {
  helix {
    selection = "chain 'A' and resseq 181:191"
  }
  helix {
    selection = "chain 'A' and resseq 192:194"
    helix_type = alpha pi *3_10 unknown
  }
  helix {
    selection = "chain 'A' and resseq 195:209"
  }
  sheet {
    first_strand = "chain 'A' and resseq 13:14"
    strand {
      selection = "chain 'A' and resseq 27:30"
      sense = parallel *antiparallel unknown
      bond_start_current = "chain 'A' and resseq 29"
      bond_start_previous = "chain 'A' and resseq 13"
    }
    strand {
      selection = "chain 'A' and resseq 156:159"
      sense = *parallel antiparallel unknown
      bond_start_current = "chain 'A' and resseq 156"
      bond_start_previous = "chain 'A' and resseq 28"
    }
    strand {
      selection = "chain 'A' and resseq 51:54"
      sense = *parallel antiparallel unknown
      bond_start_current = "chain 'A' and resseq 51"
      bond_start_previous = "chain 'A' and resseq 157"
    }
    strand {
      selection = "chain 'A' and resseq 74:77"
      sense = *parallel antiparallel unknown
      bond_start_current = "chain 'A' and resseq 74"
      bond_start_previous = "chain 'A' and resseq 52"
    }
  }
}
```

Figure 2. Equivalent `phenix.refine` parameters to Figure 1.

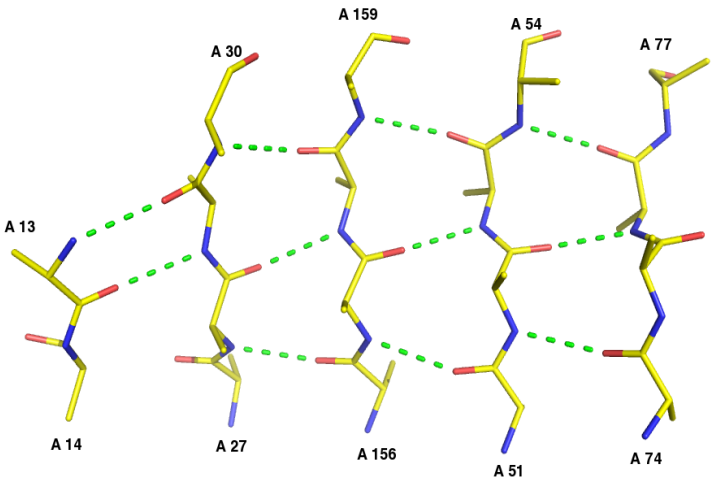

Figure 3. Beta sheet specified by the parameters in Figure 2, as rendered in *PyMOL*. (Sidechains have been omitted for clarity.) Note that not all residues annotated as belonging to strands actually form hydrogen bonds; the actual bonding pattern is dictated by the `bond_start_current` and `bond_start_previous` parameters for each strand.

`phenix.ready_set` prior to refinement to completely add hydrogens to the structure. You can also force `phenix.refine` to ignore any hydrogens present and use the implicit bonds by passing the parameter `substitute_n_for_h=True`.

All settings related to the configuration of hydrogen bonding are located in the `h_bond_restraints` block[1]. Currently, the distances used are as follows (N-O distances taken from Fabiola et al. 2002):

- explicit (H-O): 1.975 Å
- H-O outlier cutoff: 2.5 Å
- implicit (N-O): 2.9 Å
- N-O outlier cutoff: 3.5 Å

Both explicit and implicit bonds default to a sigma (standard deviation - essentially an inverse weight) of 0.05, and a slack of 0. Increasing the sigma reduces the strength of the bond restraints; increasing the slack allows it to move freely within a small range (+/- slack in either direction) before the restraint is applied. Initial experiments do not indicate any advantage to using a non-zero slack, but lower sigma values (e.g. 0.02) are beneficial in some cases, especially where explicit hydrogens are used. You may also override the global defaults and set separate sigma and slack values for each secondary structure group.

Once the hydrogen bonds have been identified, a short summary will be printed out to the log file/console:

```
109 hydrogen bonds defined.
Distribution of hydrogen bond lengths without filtering:
  2.7259 - 2.8381: 7
  2.8381 - 2.9504: 38
  2.9504 - 3.0626: 38
  3.0626 - 3.1748: 11
  3.1748 - 3.2870: 7
  3.2870 - 3.3993: 5
  3.3993 - 3.5115: 0
  3.5115 - 3.6237: 0
  3.6237 - 3.7360: 1
  3.7360 - 3.8482: 2
```

If annotation errors are present, the calculated bond lengths may cover a much wider range. For this reason, all outliers above a specified cutoff are filtered out before building the geometry restraints. Passing the parameter `remove_outliers=False` will override this, and in some instances may actually be beneficial, but we recommend visually inspecting the hydrogen bonds first to confirm that all are chemically appropriate. (This can be done in *PyMOL*; see instructions below.) After filtering, the output shown above will be repeated for the final bond list.

Nucleic acid base pairing

Version 1.6.2 adds partial support for hydrogen bond restraints between RNA base pairs (*Figure 4*) while more complete is in later nightly builds. Like *CNS* (Brünger et al. 1998), these are specified individually rather than as contiguous ranges. The automatic detection and hydrogen bond parameterization follows a similar procedure to that used for proteins, except that the all-atom contact analysis program *PROBE* (Word et al. 1999) is used to identify explicit hydrogen bonds, and a simplified list of base pairs is derived from these results. Only canonical Watson-Crick base pairs and GU pairs are supported at this time. Future versions will incorporate other known base pairings, classified according

[1] These parameters are used by both phenix.secondary_structure_restraints and phenix.refine; for the latter, the full scope name is actually refinement.secondary_structure.h_bond_restraints, but individual parameters passed as command line arguments should be recognized automatically.

to geometry as suggested by Leontis et al. (2002), versus the older Saenger (1984) Roman numeral nomenclature, which is no longer complete.

For users who require a more complete set of hydrogen bonds, we recommend the server provided by the Noller Lab at UCSC (http://rna.ucsc.edu/pdbrestraints/; Laurberg et al. 2008), which analyzes a PDB file and produces output in the custom bond format for `phenix.refine`. Note that we do not currently have any equivalent to "stacking restraints" available in *PHENIX*; additionally, although individual bases already have tight planarity restraints, the base pairs are not forced to be planar.

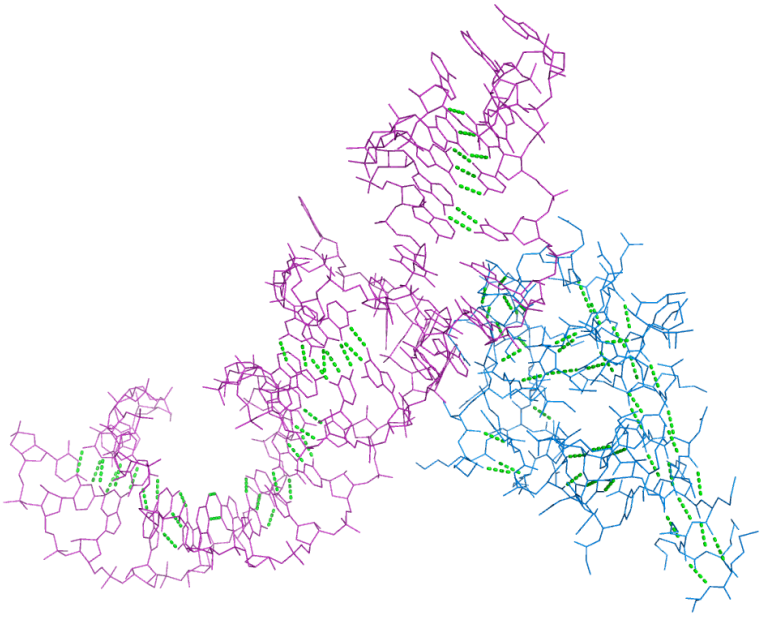

Figure 4. Automatically detected hydrogen bonds in a mixed protein-RNA structure, the signal recognition particle (PDB ID 1hq1; Batey et al. 2001).

Known limitations

The primary obstacle to generating these restraints is the difficulty of obtaining correct and complete annotations. The records in the PDB are often misleading and/or wrong; unfortunately, the annotations provided by *KSDSSP* are also occasionally incorrect. Common errors include two or more independent but adjacent helices being annotated as a single alpha helix, despite 90º bends or a 3_{10} helix in between. Both *KSDSSP* and *PROBE* are also very sensitive to input geometry, which means that poorly refined and/or manually built structures will not have all secondary structure elements detected automatically. For these situations, careful manual annotation is essential to maximize the usefulness of the added restraints. Work is underway on a graphical editor for picking secondary structures in a model (see also http://pymolwiki.org/index.php/ResDe for another approach).

At low resolution, a more serious problem is the lack of additional restraints on backbone conformation outside of regular secondary structure elements. When refining against data significantly worse than 3.0Å, Ramachandran outliers frequently comprise several percent of protein residues (0.2% is the limit recommended by Molprobity). Although `phenix.refine` does not currently offer Ramachandran restraints, version 1.6.2 introduces the separate option of restraining the model conformation to that of a high-resolution reference structure.

Additional caveats:

- No attempt is made to reconcile secondary structure restraints with NCS restraints. As always, care should be taken to exclude regions of genuine difference from NCS atom selections.
- Only bond length is restrained; angles may move freely (although in practice, other geometry restraints should limit the range of angles compatible with the specified bond length).
- Support for PDB files containing non-blank insertion codes is currently limited, especially if an insertion code occurs in the middle of a secondary structure element.
- The distribution of oxygen-nitrogen distances in beta sheets appears to be very slightly bimodal, probably due to the difference in geometry between parallel and antiparallel sheets. Increasing the slack may compensate for this, but it isn't clear whether this is necessary. Future versions may use

more intelligent distance parameters.
- Secondary structures which cross symmetry-related elements are not supported; this may occasionally happen with palindromic DNA or RNA helices. However, the custom bond syntax for `phenix.refine` may be used to manually specify hydrogen bonds.
- For extremely large structures (e.g. ribosomes), where the number of chains exceeds the number of available single-character codes, we encourage the use of two-character codes, which are also supported by Coot. However, if you prefer to use the deprecated segID, the parameters `preserve_protein_segid=True` and `preserve_nucleic_acid_segid=True` will include the segIDs in the output atom selections when identifying new secondary structure elements. (You do not need these parameters to run `phenix.refine` with the atom selections containing segIDs.)
- Detection of nucleic acid base pairs will only be run if RNA or DNA chains are identified in the PDB file. Some highly-modified RNA molecules such as tRNA may fail this procedure; for these cases, the parameter `force_nucleic_acids=True` provides a workaround.

Other uses

Two other output formats are available for the secondary structure restraints, albeit with more limited support: *PyMOL* commands for visualization (DeLano 2002), and distance restraints for *REFMAC* (Murshudov et al. 1997). A PDB file is required as input, with pre-defined atom selections optional. The same procedures described above for outlier filtering and atom selection are applied, so the final output should be identical to what would be obtained running phenix.refine with the same parameters.

- *PyMOL* format:

```
phenix.secondary_structure_restraints model.pdb \
      [restraints.eff] format=pymol > h_bonds.pml
```

- Example of output:

```
dist (chain 'A' and resi 9 and name N), (chain 'A' and resi 6 and name O)
```

- *REFMAC* format:

```
phenix.secondary_structure_restraints model.pdb \
      [restraints.eff] format=refmac > restraints.com
```

- Example of output:

```
exte dist first chain A residue 37 atom O \
      second chain A residue 41 atom N value 2.900 sigma 0.05
```

Restraints for *REFMAC* can be included as part of the input keywords; for *PyMOL*, once the PDB file is loaded distance objects can be created by selecting "Run. . ." from the "File" menu and selecting the `.pml` script, or by typing (for example) "`@/path/to/script/h_bonds.pml`" at the `PyMOL>` prompt. (For clarity, you may want to enter the command "`hide labels`" after running the script.)

Additional resources

- *KSDSSP* (included in *PHENIX* distribution):
  http://www.cgl.ucsf.edu/Overview/software.html#ksdssp
- ResDe (custom bond parameter editor for *PyMOL*):
  http://pymolwiki.org/index.php/ResDe
- Base pairing restraints generator (Noller Lab):
  http://rna.ucsc.edu/pdbrestraints/

Acknowledgements

We thank Peter Grey, Bradley Hintze, Dirk Kostrewa, and Francis Reyes for scientific discussions, Anton Vila-Sanjurjo for suggestions and code, Timm Maier for testing and feedback, and Francis Reyes and Allyn Schoeffler for sharing unpublished data. We gratefully acknowledge the *PHENIX* Industrial Consortium and NIH/NIGMS (grant P01GM063210) for financial support.

References

Adams PD, Afonine PV, Bunkóczi G, Chen VB, Davis IW, Echols N, Headd JJ, Hung LW, Kapral GJ, Grosse-Kunstleve RW, McCoy AJ, Moriarty NW, Oeffner R, Read RJ, Richardson DC, Richardson JS, Terwilliger TC, Zwart PH. PHENIX: a comprehensive Python-based system for macromolecular structure solution. *Acta Crystallogr D Biol Crystallogr*. **66**:213-21. PMID: 20124702

Afonine PV, Grosse-Kunstleve RW, Adams PD (2005). *CCP4 Newsletter.* **42**, contribution 8.

Batey RT, Sagar MB, Doudna JA. (2001) Structural and energetic analysis of RNA recognition by a universally conserved protein from the signal recognition particle. *J Mol Biol.* **307**:229-46. PMID: 11243816

Berman HM, Westbrook J, Feng Z, Gilliland G, Bhat TN, Weissig H, Shindyalov IN, Bourne PE. (2000) The Protein Data Bank. *Nucleic Acids Res.* **28**:235-42. PMID: 10592235

Bernstein FC, Koetzle TF, Williams GJB, Meyer EF Jr, Brice MD, Rodgers JR, Kennard O, Shimanouchi T, Tasumi M. (1977) The Protein Data Bank: a computer-based archival file for macromolecular structures. *J Mol. Biol.* **112**:535-42. PMID: 875032

Brünger AT, Adams PD, Clore GM, DeLano WL, Gros P, Grosse-Kunstleve RW, Jiang JS, Kuszewski J, Nilges M, Pannu NS, Read RJ, Rice LM, Simonson T, Warren GL. (1998) Crystallography & NMR system: A new software suite for macromolecular structure determination. *Acta Crystallogr D Biol Crystallogr*. **54**:905-21. PMID: 9757107

DeLano, W.L. The PyMOL Molecular Graphics System. (2008) DeLano Scientific LLC, Palo Alto, CA, USA. http://pymol.org

Fabiola F, Bertram R, Korostelev A, Chapman MS. (2002) An improved hydrogen bond potential: impact on medium resolution protein structures. *Protein Sci.* **11**:1415-23. PMID: 12021440

Grundner C, Ng HL, Alber T. (2005) Mycobacterium tuberculosis protein tyrosine phosphatase PtpB structure reveals a diverged fold and a buried active site. *Structure* **13**:1625-34. PMID: 16271885

Kabsch W, Sander C. (1983) Dictionary of protein secondary structure: pattern recognition of hydrogen-bonded and geometrical features. *Biopolymers* **22**:2577-637. PMID: 6667333

Laurberg M, Asahara H, Korostelev A, Zhu J, Trakhanov S, Noller HF. (2008) Structural basis for translation termination on the 70S ribosome. *Nature* **454**:852-7. PMID: 18596689

Leontis NB, Stombaugh J, Westof E. (2002) The non-Watson-Crick base pairs and their associated isostericity matrices. *Nucleic Acids Res.* **30**:3497-3531. PMID: 12177293

Murshudov GN, Vagin AA, Dodson EJ. (1997) Refinement of macromolecular structures by the maximum-likelihood method. *Acta Crystallogr D Biol Crystallogr.* **53**:240-55. PMID: 15299926

Saenger W. (1984) *Principles of Nucleic Acid Structure.* Springer-Verlag, New York, NY.

Word JM, Lovell SC, LaBean TH, Taylor HC, Zalis ME, Presley BK, Richardson JS, Richardson DC. (1999) Visualizing and quantifying molecular goodness-of-fit: small-probe contact dots with explicit hydrogen atoms. *J Mol Biol.* **285**:1711-33. PMID: 9917407

cctbx Spotfinder: a faster software pipeline for crystal positioning

Nicholas K. Sauter[a]

[a]*Lawrence Berkeley National Laboratory, Berkeley, CA 94720*

Correspondence email: NKSauter@LBL.Gov

Synopsis

This article documents the program `distl.signal_strength`, used to locate candidate Bragg spots on X-ray diffraction images for macromolecular crystallography. While standalone analysis requires about 3 seconds/image on typical Linux systems, an order of magnitude increase in the overall throughput can be achieved using concurrent multiprocessing within a client/server implementation. The program is thus suitable for the rapid location of the best-diffracting positions within the crystal sample using a low-dose X-ray probe.

Introduction

The development of microfocused X-ray beams at synchrotron facility endstations has made it possible to obtain higher-signal, lower mosaicity datasets from small crystal samples (Fischetti *et al.*, 2009). With small crystal dimensions of order 5 μm (matched to the diameter of present microbeams), it may be necessary to examine numerous specimens in order to assemble a complete dataset, making it highly desirable to automate the process of centering each sample in the microbeam. Various approaches have been proposed (Pothineni *et al.*, 2006; Song *et al.*, 2007), and it has been possible to automatically center the sample-holding loop (or other device) using videomicroscopy. However, it has been more difficult to visually identify small crystals within the loop, thus requiring the more robust approach of scanning the sample (translating it with respect to the microbeam), so as to collect a low-dose diffraction image at each translational position. It has been noted that such X-ray based autocentering may take up to 10 minutes for the smallest crystals (Song *et al.*, 2007), which presumably require very fine rastering to locate. This outcome could be improved dramatically by the use of a photon-counting pixel array detector such as the Pilatus-6M that supports a framing rate of 10 Hz. An accompanying challenge is to write software that can quantify the measured signal at a reasonably high turnaround rate, so that the diffraction analysis can keep pace with the rapid data acquisition needed for fine-grained coverage of the sample.

The standalone spotfinder program and client/server pair described below are meant to provide a toolbox for rapid diffraction analysis within the beamline computing environment. The software architecture is the same as described for the cctbx package (http://cctbx.sf.net; Grosse-Kunstleve *et al.*, 2002), with a high-level Python scripting interface that is meant to encourage the reuse and adaptation of code as the problems change. One example is that new detector hardware types can be readily supported as they are introduced.

Installation

The spotfinder program is bundled and distributed with the packages *LABELIT* and *PHENIX*, and can therefore be downloaded from either Web site (http://cci.lbl.gov/labelit/ or http://www.phenix-online.org/). Newest-version *PHENIX* installers are released on an almost daily basis, while *LABELIT* releases currently cycle every few months. Follow the installation instructions, and source the appropriate setup file (given in the message printed by the installer) to place the command-line dispatchers on path.

Command line reference

Use the command `distl.signal_strength` to produce a quick summary of the diffraction characteristics from a single diffraction exposure:

Usage:

```
distl.signal_strength image_filename [parameter=value [parameter2=value2
...]]
```

Example:

```
distl.signal_strength lysozyme_001.img distl.res.outer=2.0
```

Optional command line parameters change the program operation as follows (Default values are shown):

`distl.res.outer=None`

If specified, this is the outer (high) resolution limit to be used for the diffraction analysis, in Ångstroms. This option is useful for two reasons. Firstly, if a large number of images from the same crystal specimen are to be examined (in order to locate the best-diffracting position), then placing a uniform limit on the resolution range permits the number of observed Bragg spots to act as a good proxy of the diffraction strength. Secondly, areas on the image that are outside the outer resolution limit are not analyzed, potentially producing a substantial speedup in program throughput. [Note: areas on the stored image that are not part of the active detector are already excluded from analysis. Examples are the corner areas on circular image plates (such as the Mar), the inactive pixel stripes between fiber-optic tapers on CCD detectors (such as the ADSC), and the inactive pixel stripes between modules of the Pilatus detector.] Camera parameters such as the sample-to-detector distance and swing-arm angle are taken from the file header, to calculate the resolution at each pixel.

`distl.res.inner=None`

If specified, this is the inner (low) resolution limit to be used for the diffraction analysis, in Ångstroms. Excluding the low-resolution Bragg spots may be a potential workaround if there is severe beam leakage around the beam stop masquerading as a Bragg signal. However, the built-in heuristics that filter out unusually-large signal areas and very intense signals will normally exclude such artifacts anyway. The inner resolution cutoff has no effect on overall program throughput, as the filter is applied after the image is analyzed. This program option is only recommended for unusual situations.

`distl.minimum_signal_height=[1.5 for CCDs; 2.5 for pixel-array detectors]`

This parameter determines whether a given pixel is classified as background or signal. Active pixels are classified within non-overlapping 100×100-pixel tiles. For each tile, the best-fit plane is chosen to represent the background level. Pixel heights are distributed above and below this plane with a normal distribution whose standard deviation σ is readily calculated. Pixels higher than `minimum_signal_height`×σ above the background are classified as signal. Two successive rounds (now with 50×50-pixel tiles) are employed to remove the signal pixels from the background level. With CCD detectors the longstanding default of 1.5σ has been a highly successful compromise between increased sensitivity (favoring a lower cutoff) and better noise discrimination (favoring a higher cutoff; any cutoff lower than 1.25σ produces numerous false Bragg spots). For pixel-array detectors, which lack any significant point-spread function, 2.5σ gives better results and is now the pixel-array default. Images from very long unit cells (viruses, ribosomes) potentially have close spots that run into each other, without being separated down to the baseline. The heuristic rules in `distl` will reject these close signals, and in severe cases this will interfere with the ability to index the lattice. The solution is to raise the cutoff level to as high as 5σ, thus correctly separating the close spots. It is therefore important to consider raising the `minimum_signal_height` if the crystals have a large unit cell. At present there is no automatic way to do this; the program has no way to know the cell length ahead of time. In the future it will be beneficial to add some preliminary noise analysis to provide more sophisticated guidance for spot detection.

```
distl.minimum_spot_area=None [5 for pixel-array detectors, 10 otherwise]
```

If specified, this is the minimum number of contiguous pixels that is considered to be a spot. For image plate and CCD detectors the hard-coded default is 10 pixels/spot. With pixel-array technology, spots are much narrower due to the sharp point-spread function, but they are still generally distributed over a few pixels. The pixel-array default is therefore set to 5 pixels/spot. Synchrotron beamlines experimenting with new detectors or optics should test this parameter to find the optimum setting!

```
verbose=False
```

If True, the program will output detailed statistics on all Bragg spots and show signal pixel locations. This is potentially useful for beamline commissioning.

```
pdf_output=None
```

If specified, this is the filename (*.pdf) for an optional PDF-format graphical output showing the image and associated Bragg signals. This visual output is the most direct way to understand the "big picture" of what the program results mean. Comparing one's own visual impression of the diffraction image with the marked up spotfinder results will reveal whether the program has missed real Bragg spots (false negatives) or overinterpreted bad signals (false positives). The contrast level is pre-set internally. Pink stripes are used to color-code the inactive areas between detector modules (for the Pilatus), and red squares (again for the Pilatus) are inactive pixels, which should be the same on every image for a given instrument. Within Bragg spots, color circles indicate that the spot has been tagged as a "good Bragg spot candidate" (see below). Pink circles tag the position of the maximum pixel, and red circles show the spot center of mass.

```
--help
```

Produces an informative program synopsis.

Program operation and output

Computational steps performed by the program have already been described in several publications (Zhang *et al.*, 2006; Sauter *et al.*, 2004; Sauter & Zwart, 2009; Sauter & Poon, 2010). Typical results written to *stdout* are as follows:

```
                    File : 0_clmtr_edge_403.cbf
              Spot Total :    177
    In-Resolution Total :    170
  Good Bragg Candidates :    157
             Ice Rings :      1
    Method 1 Resolution :   2.55
    Method 2 Resolution :   2.08
      Maximum unit cell :  108.9
%Saturation, Top 50 Peaks :   0.09
In-Resolution Ovrld Spots :      0

Bin population cutoff for method 2 resolution: 20%

Number of focus spots on image #403 within the input resolution range: 170
Total integrated signal, pixel-ADC units above local background (just the good Bragg candidates) 147322
Signals range from 37.2 to 11773.1 with mean integrated signal 997.2
Saturations range from 0.0% to 0.7% with mean saturation 0.0%
```

Three types of spot count are listed:

- "Spot Total" is the number of separate spots that rise above the minimum thresholds for signal height and spot area. A graph of average pixel intensity vs. resolution is examined to prefilter likely ice rings.
- "In-Resolution Total" is the subset remaining after high- and low-resolution filters are applied. The command-line distl.res filter is applied here (if given), as well as the "Method 2 Resolution" filter described below.
- "Good Bragg Candidates" are the spots remaining after the application of several spot-quality heuristics:
    - A histogram of spot count vs. resolution is used to implement a second filter for ice rings.
    - Spots with ill-defined profiles having more than two signal maxima are not counted.
    - Outliers in intensity, area, eccentricity and skewness are thrown away.
    - Spots with too-close nearest neighbors are filtered.

Limiting resolution is estimated by the two methods defined in Zhang *et al.* (2006). Method 2 is used to choose spots for *LABELIT* autoindexing. It relies on the ability to produce a histogram of spot count vs. resolution, and therefore requires a minimum number of spots (usually 25). The resolution cutoff is determined by noting the falloff in bin population at higher diffraction angles. The maximum unit cell is estimated by observing nearest-neighbor distances and assuming that the closest spacing corresponds to the largest unit cell length.

"In-resolution" spots are used to produce several signal strength metrics: "% Saturation", "In-Resolution Overloaded Spots", "Signals range" and "Saturations range".

A final "Total integrated signal" metric is computed on the "Good Bragg Candidates". This value is the summed signal height (corrected for background) over all signal pixels. ADC units are analog-to-digital units, as recorded in the raw image file.

Performance assessment for crystal positioning

To position the crystal optimally in the beam, we aim to translate the sample to the position that maximizes the total number of good Bragg spots, or average intensity of Bragg spots, within a given resolution range. Low-dose X-rays can be used to perform this raster scan over the sample, as described (Song *et al.*, 2007). Very high throughput is achieved with shutterless exposures using a Pilatus-6M detector. However, the resulting turnaround time of about 0.2 seconds/image places very high performance requirements on the computational pipeline; which typically takes about 3 seconds to process one image. The magnitude of the challenge can be assessed by profiling the spotfinding code, as is done here with a 64-bit, 2.9 GHz Xeon machine running Fedora Core 8. The processor was equipped with 32 GB RAM and 16 CPU cores, although only one core was used by the single-threaded spotfinder process:

Computational step	Typical time/image	Comments
Load the dynamic libraries	0.50 sec	Client/server removes this overhead
Read file from NFS disk	0.70 sec	Local file I/O takes only 0.04 sec
Uncompress CBF image to memory	0.27 sec	cctbx-optimized code takes only 0.09 sec
Classify pixels: background/signal	0.63 sec	
First ice ring filter	0.23 sec	
Find all spots	0.14 sec	
Second ice ring filter	0.15 sec	
Additional heuristics for good spots	0.15 sec	
Total time:	2.77 sec	

Client-server architecture

The above-listed performance data show that an order-of-magnitude improvement is needed to keep pace with Pilatus-6M acquisition. We therefore move to a client-server architecture that eliminates the need to reload the dynamic libraries for each image (since the server process is persistent), and runs with multiple processes, so that numerous images may be processed concurrently within separate cores. At present, 16-core CPUs are available for under $6000, so they are within reach of beamline operating budgets. With this scheme it is easy to achieve the desired 0.2 second/image total throughput.

Server:

```
distl.mp_spotfinder_server_read_file [parameter=value ... ]
```

The program operates as a multithreaded server. Allowed parameters are:

- `distl.port=8125` (Required) The server will listen for requests on this port.
- `distl.processors=1` (Required) The total number of processes to be forked to listen for requests.
- `distl.minimum_spot_area=` same as above, the minimum spot area in pixels.
- `distl.minimum_signal_height=` same as above, the minimum signal height.
- `distl.res.outer=` same as above, the outer resolution limit in Ångstroms.

Client:

```
distl.thin_client <filepath> <host> <port>
```

No keyword parameters are allowed. The client simply takes the filepath (must be a valid filepath on the server machine), host name (usually "localhost") and port number, and outputs the spot analysis to *stdout*.

Notes:

The server can be killed from the command line by Ctrl-C, or via the client by sending the message:

```
distl.thin_client EXIT <host> <port>
```

While the server is supposed to queue requests, too many at once can cause some requests to drop out, in a manner that is not fully characterized. Therefore in the example given (`<path to sources>/spotfinder/servers/thin_client.csh`), a `/bin/sleep` command is used to time the requests at a reasonable pace given the particular server host and number of processes. In application, it is the responsibility of the caller (the beamline data collection process) to avoid overloading the server with too many simultaneous requests.

LABELIT contains a separate program (`labelit.distl`) to perform a similar spot finding function for use in autoindexing. That implementation is not suitable for multiprocessing because it writes the spot list to disk in the current working directory under a constant file name. The file can be erased with the command `labelit.reset`.

In contrast, `distl.signal_strength` and `distl.mp_spotfinder_server_read_file` perform all work in memory without any file output.

Results

Low-dose exposures were used to probe samples on a 5 × 6-position grid (Diamond, ADSC detector) or a

5 × 5-position grid (SSRL, Pilatus-6M). Images were visually inspected to produce a subjective rank for each exposure, taking into account factors such as the limiting resolution and strength of the Bragg spots. Separately, the images were analyzed with the automated spotfinder process, using an up-front resolution limit (`distl.res.outer`) of 3.0 Å.

An automated ranking scheme was developed that is consistent with the subjective rank from visual inspection. The 30 or 25 images from each sample are ranked by two criteria, the "Total Integrated Signal" in pixel-ADC units, and the count of "Good Bragg Candidates", and the rank scores based on these two criteria are averaged with equal weight. If two images receive the same average score, the tie is broken by giving a higher priority to "Total Integrated Signal". No score is developed unless there is a numerical score for "Method 2 Resolution" (although the resolution isn't actually included in the ranking); therefore images with too few spots are not scored.

Application programming interface

The spotfinder software can be accessed directly through Python code. Although the necessary interface is not formally documented, example usage is given by the program itself, within the `<path to sources>/spotfinder/` directory:

`./command_line/signal_strength.py`: Illustrates the use of command-line parameters.

`./applications/signal_strength.py`: Illustrates the core function calls, as well as the detailed parsing of the resulting spot list.

Acknowledgments

Numerous contributions from synchrotron groups helped to shape this software. Test results were contributed by Michael Soltis, Ana González and Penjit (Boom) Moorhead (Stanford Synchrotron Radiation Lightsource); Craig Ogata, Mark Hilgart and Sudhir Pothineni (GM/CA-CAT, Advanced Photon Source); John Skinner and Annie Heroux (National Synchrotron Light Source); and Alan Ashtun, Katherine McAuley, Graeme Winter and Mark Williams (Diamond Light Source, Ltd., UK). Herbert Bernstein (Dowling College) offered his expertise toward the optimization of CBF decompression, and Chris Nielson (Area Detector Systems Corp.) engaged in valuable discussions. Ralf Grosse-Kunstleve at LBNL helped to implement the overall software architecture. The financial support of NIH/NIGMS under grant number R01GM077071 is gratefully acknowledged. The work was partly supported by the US Department of Energy under Contract No. DE-AC02-05CH11231.

References

Fischetti, R.F., Xu, S., Yoder, D.W., Becker, M., Nagarajan, V., Sanishvili, R., Hilgart, M.C., Stepanov, S., Makarov, O. & Smith, J.L. (2009). Mini-beam collimator enables microcrystallography experiments on standard beamlines. *J. Synchrotron Rad.* **16**, 217-225.

Grosse-Kunstleve, R.W., Sauter, N.K., Moriarty, N.W. & Adams, P.D. (2002). The Computational Crystallography Toolbox: crystallographic algorithms in a reusable software framework. *J. Appl. Cryst.* **35**, 126-136.

Poon, B.K., Grosse-Kunstleve, R.W., Zwart, P.H. & Sauter, N.K. (2010). Detection and correction of underassigned rotational symmetry prior to structure deposition. *Acta Cryst.* D**66**, 503-513.

Pothineni, S.B., Strutz, T. & Lamzin, V.S. (2006). Automated detection and centring of cryocooled protein crystals. *Acta Cryst.* D**62**, 1358-1368.

Sauter, N.K., Grosse-Kunstleve, R.W. & Adams, P.D. (2004). Robust indexing for automatic data collection. *J. Appl. Cryst.* **37,** 399-409.

Sauter, N.K. & Zwart, P.H. (2009). Autoindexing the diffraction patterns from crystals with a pseudotranslation. *Acta Cryst.* D**65**, 553-559.

Sauter, N.K. & Poon, B.K. (2010). Autoindexing with outlier rejection and identification of superimposed lattices. *J. Appl. Cryst.* **43**, 611-616.

Song, J., Mathew, D., Jacob, S.A., Corbett, L., Moorhead, P. & Soltis, S.M. (2007). Diffraction-based automated crystal centering. *J. Synchrotron Rad.* **14**, 191-195.

Zhang, Z., Sauter, N.K., van den Bedem, H., Snell, G., and Deacon, A.M. (2006). Automated diffraction image analysis and spot searching for high-throughput crystal screening. *J. Appl. Cryst.* **39**, 112-119.

Atomic Displacement Parameters (ADPs), their parameterization and refinement in PHENIX

Pavel V. Afonine,[a] Alexandre Urzhumtsev,[b,c] Ralf W. Grosse-Kunstleve[a] and Paul D. Adams[a,d]

[a]*Lawrence Berkeley National Laboratory, Berkeley, CA 94720*
[b]*IGBMC, CNRS-INSERM-UdS, 1 rue Laurent Fries, B.P.10142, 67404 Illkirch, France*
[c]*Université Nancy; Département de Physique - Nancy 1, B.P. 239, Faculté des Sciences et des Technologies, 54506 Vandoeuvre-lès-Nancy, France.*
[d]*Department of Bioengineering, University of California at Berkeley, Berkeley, CA 94720*

Correspondence email: PAfonine@LBL.Gov

Introduction

This article describes the parameterization of, and refinement procedures for, Atomic Displacement Parameters (ADPs, or *B*-factors), as they are implemented in the crystallographic structure refinement program `phenix.refine` (Afonine *et al.*, 2005). The algorithms and parameterizations are implemented using an object oriented library approach and thus can be re-used in different contexts.

1. Atomic Displacement Parameters

Diffraction experiments produce data representing time- and space-averaged images of the crystal structure: time-averaged because atoms are in continuous thermal motions around mean positions, and space-averaged because there are often small differences between symmetry copies of the asymmetric unit in a crystal, especially in the case of macromolecular crystals. The dynamic displacements and the static spatial disorder lead to vanishing high-resolution data in reciprocal space and blurring of the diffracting density (electron or nuclear) in real-space. Ignoring the displacements when modeling the diffraction experiment would lead to a poor fit of the calculated data to the observed data. Modeling of the *small* dynamic displacements as isotropic or anisotropic harmonic displacements has been a standard practice from the earliest days of crystallography. *Larger* displacements (beyond harmonic approximation) can be modeled by using an anharmonic model (Gram-Charlier expansion; Johnson & Levy, 1974; Kendal & Stuart, 1958; not available in `phenix.refine`) or "alternative conformations".

The atomic displacement is a superposition of a number of contributions (Dunitz & White, 1973; Prince & Finger, 1973; Johnson, 1980; Sheriff & Hendrickson, 1987; Winn *et al.*, 2001), such as:

- Local atomic vibration
- Motion due to a rotational degree of freedom (e.g. libration around a torsion bond)
- Loop or domain movement
- Whole molecule movement
- Crystal lattice vibrations

More detailed models can be envisioned, but in practice many of today's refinement programs use an approximation and separate the total ADP, $\mathbf{U}_{\mathrm{TOTAL}}$, into three components:

$$\mathbf{U}_{\mathrm{TOTAL}} = \mathbf{U}_{\mathrm{CRYST}} + \mathbf{U}_{\mathrm{GROUP}} + \mathbf{U}_{\mathrm{LOCAL}} \qquad (1)$$

While the individual members of (1) represent different kinds of displacements, each of them can be modeled with different accuracy or using different models. For example, local atomic vibration, $\mathbf{U}_{\mathrm{LOCAL}}$, can be modeled using a less detailed, isotropic, model that uses only one parameter per atom. A more detailed (and accurate) anisotropic parameterization uses six parameters but requires more experimental observations to be practical. Group atomic displacement, $\mathbf{U}_{\mathrm{GROUP}}$, can be modeled using the TLS parameterization ($\mathbf{U}_{\mathrm{TLS}}$) or just one parameter per group of atoms (Fig. 1).

There are a relatively large number of conventions and notations used in connection with ADPs (**B**, **U**, $\mathbf{U}^{*}$, $\mathbf{U}_{\mathrm{CART}}$, $\mathbf{U}_{\mathrm{CIF}}$, etc); see Grosse-Kunstleve & Adams (2002) for a comprehensive review. In what follows we consistently use **U** assuming that the appropriate convention is used based on the context.

2. U_{CRYST}

$\mathbf{U}_{CRYST}$ (a symmetric 3x3 matrix) models the common displacement of the crystal (lattice vibrations) as a whole and some additional experimental anisotropic effects (Sheriff & Hendrickson, 1987; Usón *et al.*, 1999). This contribution is exactly the same for all atoms and thus it possible to treat this effect directly while performing overall anisotropic scaling (Afonine *et al.*, 2005) to compute the total model structure factors

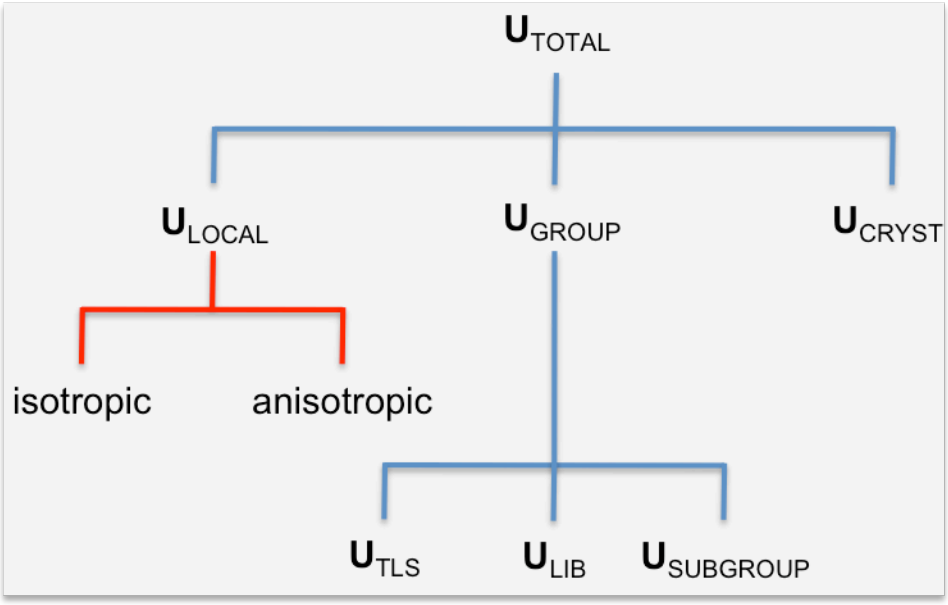

Figure 1. Hierarchy of contributions to atomic displacement parameter.

$$\mathbf{F}_{model} = k_{overall} \exp\left(-\frac{\mathbf{h}^t \mathbf{U}_{cryst} \mathbf{h}}{4}\right)\left(\mathbf{F}_{calc} + k_{sol} \exp\left(-\frac{B_{sol} s^2}{4}\right)\mathbf{F}_{mask}\right) \quad (2)$$

$\mathbf{U}_{CRYST}$ is forced to obey the crystal symmetry constraints. `phenix.refine` reports refined elements of $\mathbf{U}_{CRYST}$ matrix expressed in a Cartesian basis and uses the $\mathbf{B}_{CART}$ notation (for details, see Grosse-Kunstleve & Adams; 2002).

3. U_{GROUP}

$\mathbf{U}_{GROUP}$ is intended to model the contribution to $\mathbf{U}_{TOTAL}$ arising from concerted motions of multiple atoms (group motions). It allows for the combination of group motion at different levels (for example, *whole molecule + chain + residue*) and for the use of models of different degrees of sophistication (or accuracy), such as general TLS, TLS for a fixed axis (a librational ADP; $\mathbf{U}_{LIB}$), and a simple group isotropic model with one single parameter. In its most general form, $\mathbf{U}_{GROUP}$ can be $\mathbf{U}_{TLS}$ + $\mathbf{U}_{LIB}$ + $\mathbf{U}_{SUBGROUP}$, where, for example, $\mathbf{U}_{TLS}$ would model the motion of the whole molecule or a large domain, $\mathbf{U}_{SUBGROUP}$ would model the displacement of a smaller group such as a chain using a simpler one-parameter model and $\mathbf{U}_{LIB}$ would model a side chain libration around a torsion bond using a simplified TLS model (Stuart & Phillips, 1985). Depending on the context (model and data quality), not all these components can be realized. For example, $\mathbf{U}_{GROUP}$ may be just $\mathbf{U}_{TLS}$ or $\mathbf{U}_{SUBGROUP}$. Nested TLS parameterization (when a smaller TLS group can be enclosed within a larger TLS group) is not yet implemented in `phenix.refine`.

3.1. $U_{SUBGROUP}$

$\mathbf{U}_{SUBGROUP}$ represents one refinable isotropic ADP per group of selected atoms, with any number of groups. In `phenix.refine` there are two pre-defined selections for $\mathbf{U}_{SUBGROUP}$ to refine one or two (side+main chain atoms) $\mathbf{U}_{SUBGROUP}$ per residue. An arbitrarily selected set of atoms can also be a group. There is no general rule for choosing one parameterization over another; the choice depends on the resolution (data-to-parameter ratio) and is usually made by systematic testing using R_{work} and R_{free} as the criteria. No restraints are applied to $\mathbf{U}_{SUBGROUP}$, but the value can be constrained between predefined minimum and maximum values.

3.2. U_{LIB}

This is a special case of the TLS parameterization for a rigid-body motion that occurs around a fixed axis (see for example: Dunitz & White, 1973; Stuart & Phillips, 1985). An example of such motion could be a libration of a flexible amino-acid side chain around a bond vector (such as the C_α-C_β torsion bond. Currently this approach is being implemented in `phenix.refine`.

3.3. U_{TLS}

If the TLS model is used for the rigid-body motion of a group of atoms then

$$\mathbf{U}_{TLS} = \mathbf{T} + \mathbf{A}\mathbf{L}\mathbf{A}^t + \mathbf{A}\mathbf{S} + \mathbf{S}^t\mathbf{A}^t \quad (3)$$

with 20 refinable **T** (translation), **L** (libration) and **S** (screw-rotation) matrix elements per group (Schomaker & Trueblood; 1968).

The choice of TLS groups is often subjective and may be based on visual inspection of the molecule in an attempt to identify distinct and potentially independent fragments. A more rigorous approach is implemented in the TLSMD algorithm (Painter & Merritt, 2006a, 2006b)). The TLSMD algorithm identifies TLS groups by splitting a whole molecule into smaller pieces followed by fitting of TLS parameters to the previously refined atomic *B*-factors for each piece. Therefore, it is very important that the input ADP values for the TLSMD procedure are minimally biased by the restraints used in previous refinements, and meaningful in general (not reset to an arbitrary constant value, for example). Ideally, one may need to perform a round of unrestrained ADP refinement just for the purpose of TLS group identification with TLSMD. Since an unrestrained refinement may not be stable (it might produce non-physical values or a large spread of refined *B*-factors, especially at lower resolution), it might be better to perform a group *B*-factor refinement only, using one or two refinable parameters per residue. Such a refinement will not make use of any ADP restraints and therefore yields refined *B*-factors that attempt to fit the data most closely within the limits of the group definition used. Futhermore, currently the TLSMD procedure does not generate a unique definitive answer for the TLS group selection but rather gives a list of possible choices and the researcher has to make the decision to test one or more TLS group selections; this still leads to an element of subjectivity in the definition of TLS groups.

3.4. U_{LOCAL}

$\mathbf{U}_{LOCAL}$ models harmonic atomic vibrations occurring around the mean atomic position. Depending on the experimental data quality, this can be a simple isotropic model where the atomic vibrations have equal amplitude in all directions, or it can be more complex where atomic vibration is assumed to be anisotropic. Ideally, if all the group (or global) contributions to the total atomic displacement are subtracted, leaving only the local atomic vibration $\mathbf{U}_{LOCAL}$, then it should obey Hirshfeld's rigid bond postulate (Hirshfeld, 1976) providing a basis for the use of similarity

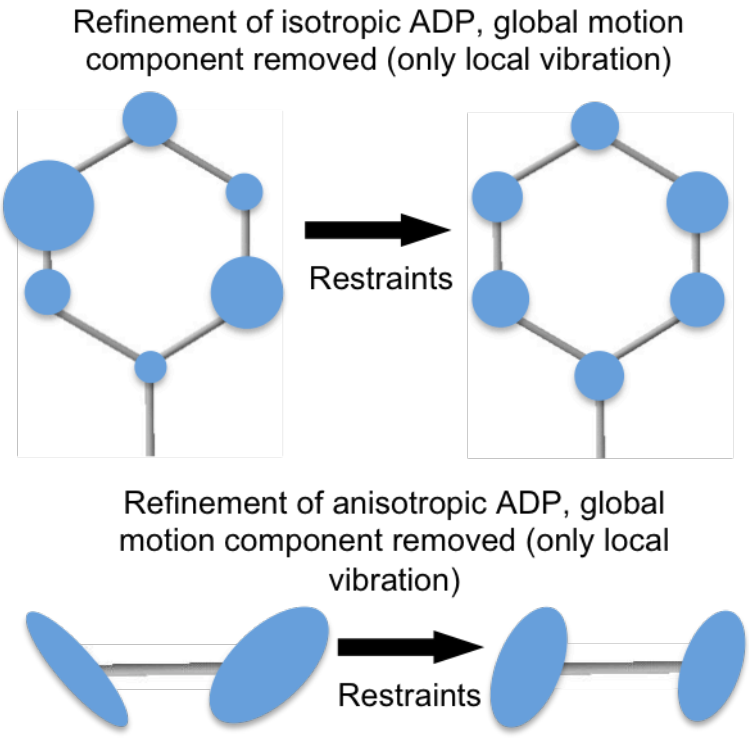

Figure 2. Illustration of similarity restraints.

restraints (Fig. 2). For isotropic ADPs:

$$T_{\text{adp}} = \sum_{\substack{\text{pairs of}\\ \text{bonded}\\ \text{atoms (i,j)}}} \left(U_{\text{local},i} - U_{\text{local},j}\right)^2 \qquad (4)$$

and for anisotropic ADPs:

$$T_{\text{adp}} = \sum_{\substack{\text{pairs of}\\ \text{bonded}\\ \text{atoms (i,j)}}} \sum_{k=1}^{6} \left(U^k_{\text{local},i} - U^k_{\text{local},j}\right)^2 \qquad (5)$$

which is similar to (4) where the inner sum spans over all six ADP matrix elements. Despite its simplicity this formula has proved useful in many cases. However, more sophisticated approaches have been suggested in order to better handle a number of special cases for which (5) is suboptimal (Hendrickson, 1985; Schneider, 1996; Sheldrick & Schneider, 1997). Since `phenix.refine` allows for a mixture of atoms with isotropic or anisotropic ADPs, it may happen (at least theoretically) that an isotropic atom is bonded to one having an anisotropic ADP. Currently, in this case only the isotropic component of each of the two atoms is participating in the restraint.

4. Practice: mixing contributions into U_{TOTAL}, restraints

4.1. $U_{TOTAL} = U_{CRYST} + U_{LOCAL}$

In practice, it is still customary to have one isotropic refinable parameter per atom at typical 'macromolecular' resolutions (~1.7-3.0Å), that is $\mathbf{U}_{TOTAL} = \mathbf{U}_{CRYST} + \mathbf{U}_{LOCAL}$, where the $\mathbf{U}_{GROUP}$ contribution is accumulated into other atomic parameters, including $\mathbf{U}_{CRYST}$ and $\mathbf{U}_{LOCAL}$.

Since in this case $\mathbf{U}_{LOCAL}$ contains other contributions to displacements ($\mathbf{U}_{GROUP}$) this in turn invalidates the use of restraints (4-5) (see Fig. 3 for an illustration). Although Fig. 3 contains some elements of dramatization and the actual deviations from similarity may not be as large as shown (especially for covalently bonded atoms), still in this case forcing the *B*-factors to be nearly identical is less valid. A possible work-around is to use a knowledge-based type of restraint introduced by Tronrud (1996). However, in `phenix.refine` we have implemented a 'softer' algorithm for similarity restraints, which is based on the following assumptions:

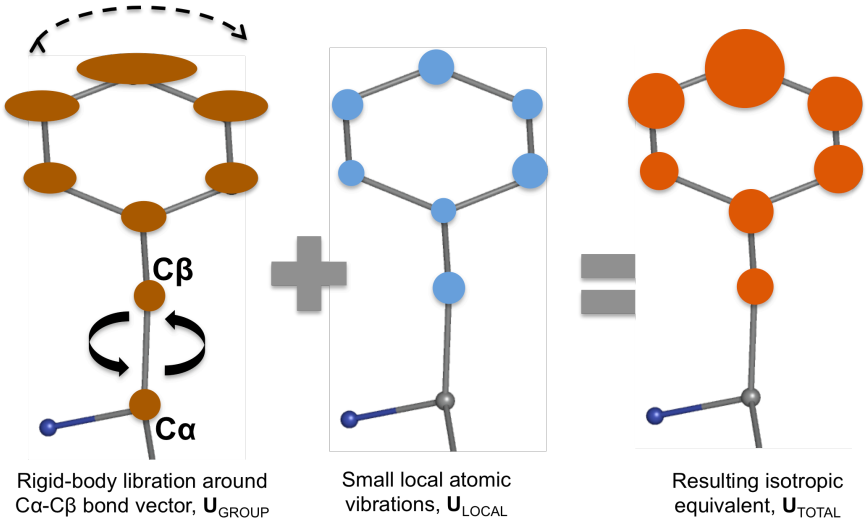

Figure 3. While local atomic vibrations ($\mathbf{U}_{LOCAL}$ obey similarity restraints, the total ADP ($\mathbf{U}_{TOTAL}$) may not obey similarity restrains because the contribution ($\mathbf{U}_{GROUP}$) arising from rigid-body motion of a whole fragment may add different displacements to each atom.

- A bond is almost rigid, therefore the ADPs of bonded atoms ($\mathbf{U}_{LOCAL}$ component) are similar (Hirshfeld, 1976);
- ADP values of spatially close (including non-bonded) atoms are similar (Schneider, 1996);

- The difference between the ADP values of atoms close in space is related to the absolute values of the ADP values. Atoms with higher ADP values are allowed larger differences (Ian Tickle, CCP4 Bulletin Board, letter from March 14, 2003).

Considering the above assumptions, we obtain

$$T_{\text{adp}} = \sum_{i=1}^{N_{\text{atoms}}} \left[\sum_{j=1}^{M_{\text{atoms}}} \frac{1}{r_{ij}^{p}} \frac{\left(U_{\text{local},i} - U_{\text{local},j}\right)^2}{\left(U_{\text{local},i} + U_{\text{local},j}\right)^{q}} \right] \qquad (6)$$

Here N_{atoms} is the total number of atoms in the model, the inner sum is extended over all M_{atoms} in the sphere of radius R around atom i, r_{ij} is the distance between two atoms i and j, $U_{\text{local},i}$ and $U_{\text{local},j}$ are the corresponding isotropic ADP values, p and q are empirical constants. By default, R, p and q are fixed at empirically derived values: 5.0Å, 1.69 and 1.03, respectively, but they can also be changed by the user. The function reduces to formula (4) if $p = q = 0$, and the radius R is set to be approximately equal to the upper limit of a typical bond length.

At high enough resolution, approximately better than 1.6-1.7Å, $\mathbf{U}_{\text{GROUP}} = \mathbf{U}_{\text{TLS}}$ is not used (currently is not implemented in `phenix.refine`) leaving $\mathbf{U}_{\text{TOTAL}} = \mathbf{U}_{\text{CRYST}} + \mathbf{U}_{\text{LOCAL}}$ where the $\mathbf{U}_{\text{LOCAL}}$ can be anisotropic.

4.2. $U_{TOTAL} = U_{CRYST} + U_{GROUP} + U_{LOCAL}$

This is the most advanced formulation of ADP parameterization available in `phenix.refine`. In this case currently $\mathbf{U}_{\text{LOCAL}}$ can only be refined isotopically for those atoms that participate in a TLS group. The NCS restraints (if available and used) as well as (4) are applied to $\mathbf{U}_{\text{LOCAL}}$ only and not to the whole ADP, $\mathbf{U}_{\text{TOTAL}}$.

`phenix.refine` allows any combination of the above ADP refinement strategies to be applied to any selected part of the structure. The only exception (which is a technical limitation and might be changed in the future) is that an atom cannot be in a TLS group and simultaneously have an anisotropic $\mathbf{U}_{\text{LOCAL}}$.

It is important to note that the positive definiteness of $\mathbf{U}_{\text{TOTAL}}$ is ensured at all times, while the individual components may or may not be positive definite (except $\mathbf{U}_{\text{CRYST}}$, see below). For example, in combined TLS and individual ADP refinement ($\mathbf{U}_{\text{TOTAL}} = \mathbf{U}_{\text{CRYST}} + \mathbf{U}_{\text{GROUP}} + \mathbf{U}_{\text{LOCAL}}$), $\mathbf{U}_{\text{LOCAL}}$ are not forced to be non-zero or even positive and $\mathbf{U}_{\text{TLS}}$ are not forced to be positive definite either, while $\mathbf{U}_{\text{TOTAL}}$ is assured to be positive definite (by using eigenvalue filtering). The benefit of such an approach is that it can compensate for non-optimal choices of TLS groups (discussed above) by a corresponding adjustment of $\mathbf{U}_{\text{LOCAL}}$ (which in *such cases* becomes a compensation factor and has little physical meaning), while the resulting overall *B*-factor, $\mathbf{U}_{\text{TOTAL}}$, is still positive definite. $\mathbf{U}_{\text{CRYST}}$ is an exception, and the physical correctness and compatibility with the crystal symmetry are enforced at

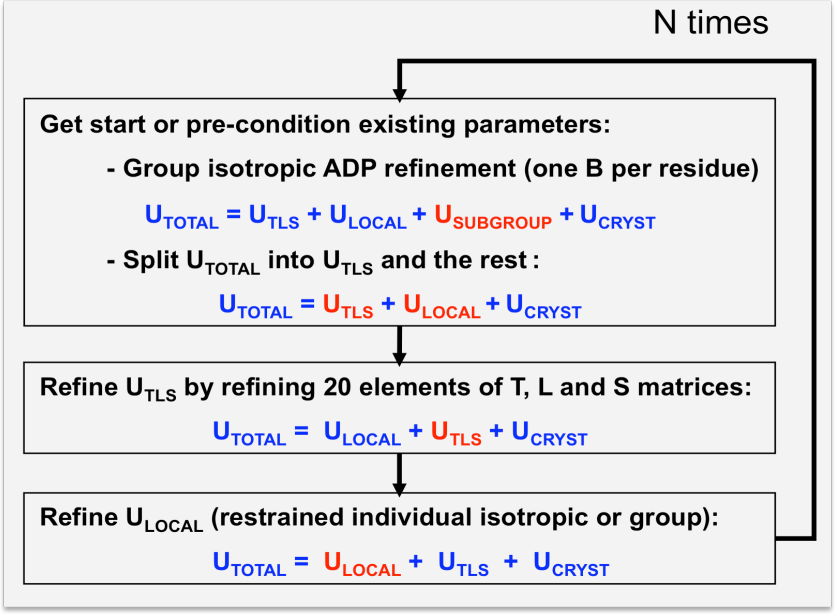

Figure 4. Protocol of combined TLS and individual ADP refinement.

the bulk-solvent correction and anisotropic scaling step.

The contributions $\mathbf{U}_{CRYST}$, $\mathbf{U}_{GROUP}$ and $\mathbf{U}_{LOCAL}$ in (1) are highly correlated making it generally impractical to separate them. In addition, when refined simultaneously the elements of the **T**, **L** and **S** matrices appear to be correlated as well. This can generate a number of numerical issues, such as: refinement of TLS matrices to non-physical values, refinement becoming stalled, and strong dependence of the final refined values on the starting values. To overcome these issues we developed a complex algorithm for efficient refinement of the terms in $\mathbf{U}_{TOTAL}$; the details are outlined at Fig. 4. The procedure begins with obtaining sensible initial values for TLS parameters and $\mathbf{U}_{LOCAL}$. This is performed in three stages: 1) pre-conditioning of *B*-factors by performing a preliminary group ADP refinement, 2) extracting **T** matrix from these refined values as described by Afonine & Urzhumtsev (2007) and 3) least-squares fit of the **T**, **L** and **S** matrices to $\mathbf{U}_{TOTAL}$ starting with the **T** matrix obtained from the previous step and zero or previously refined **L** and **S** matrices. The fitted TLS matrices are now the starting point for the TLS refinement against crystallographic data in the second step. Finally, the individual *B*-factors are refined keeping all other components fixed. This is repeated several times (3 by default).

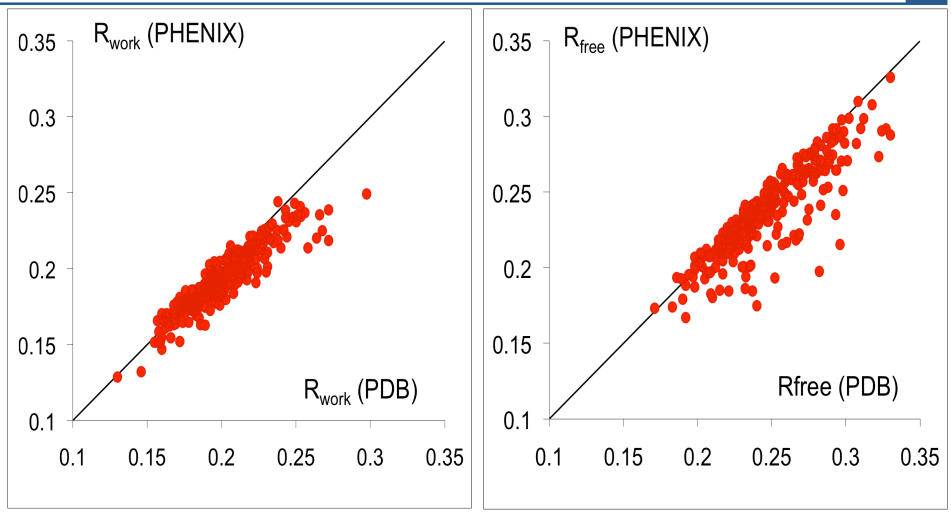

Figure 5. Result of automatic re-refinement of 355 TLS containing structures in PDB.

This combined ADP refinement protocol was tested on 355 structures from PDB that contained TLS records. The structures were selected using the strict criteria: correct TLS selections and *R*-factors reproducible within 0.5%. For the test purposes the original *B*-factors in these structures were all re-set to the model average value. The re-refinement of ADP values using the protocol described above resulted in comparable or better (than reported) final *R*-factors (Fig. 5). There was no case where refinement showed any numerical problems.

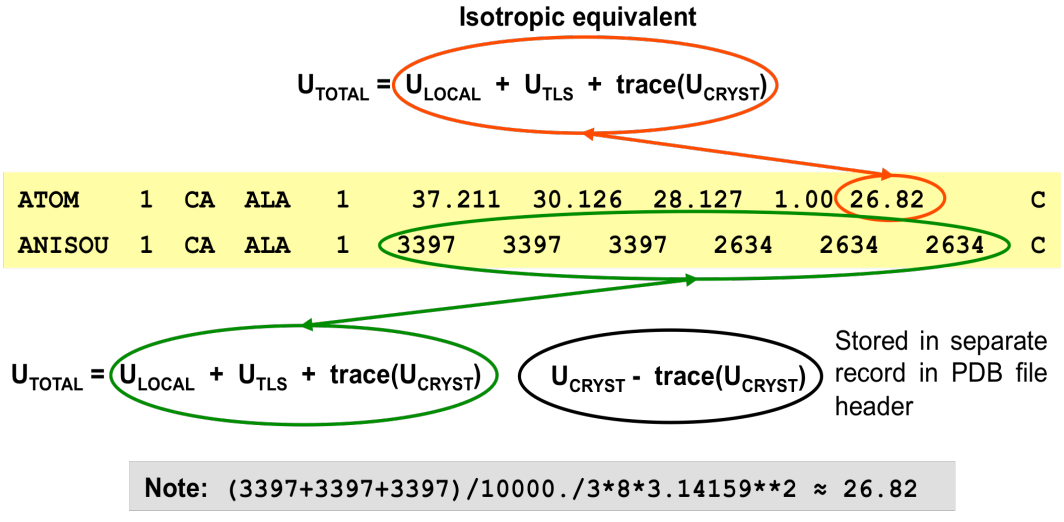

Figure 6. A scheme showing how the refined ADPs are stored in a PDB file.

5. Output of ADP information in PDB files

It should be noted that each atom participating in a TLS group receives an anisotropic ADP (ANISOU card in PDB) (Fig. 6). `phenix.refine` always outputs the total ADP for each atom to the PDB file. An exception is made for $\mathbf{U}_{\mathrm{CRYST}}$, where, similarly to CNS (Brunger, 2007), only the trace of this matrix (or the component that keeps the ADP values positive definite) is added into the output ADP for ATOM and ANISOU records, while its anisotropic component is separated and is reported in the PDB file header. To analyze the separate contributions $\mathbf{U}_{\mathrm{TLS}}$ and $\mathbf{U}_{\mathrm{LOCAL}}$ given $\mathbf{U}_{\mathrm{TOTAL}}$, `phenix.tls` (Afonine, unpublished) is a tool within *PHENIX* that is specifically designed for this.

6. Examples

In this section we illustrate the use of refinement strategies with different choices of ADP parameterization.

All refinements included five macro-cycles of individual coordinates, ADP and occupancy refinement (see the `phenix.refine` documentation for details of occupancy refinement), ordered solvent (water) update (adding, removing, refinement; data resolution permitting). If NCS is available, then both `phenix.refine` runs were performed: with and without using NCS, where the NCS groups were selected by `phenix.refine` automatically. The X-ray target weight was automatically optimized in all refinement runs. The only variation between refinement runs was the ADP parameterization:

- individual (I),
- group with one isotropic ADP per residue (G1),
- group with two isotropic ADP per residue (G2; one per main and one per side chain atoms);
- TLS only (T);
- TLS in combination with G1 (T+G1);
- TLS in combination with G2 (T+G2);
- TLS in combination with I (T+I).

In the examples below the best re-refinement result achieved in `phenix.refine` is shown in bold in the corresponding table.

Example 1: PDB code 1BL8, resolution 3.2Å

This structure was originally refined to R_{work} = 28.0 and R_{free} = 29.0% (Doyle *et al.*, 1998). Chen *et al.* (2007) re-refined this model using a Normal Mode parameterization in refinement, reducing the *R*-factors to 27.2 and 27.2%, respectively (leaving no gap between R_{work} and R_{free}). At this resolution automated water model updates were not possible.

R_{work} / R_{free} (%)	Refinement strategy							
	I	I+NCS	G1+NCS	G2+NCS	T+NCS	T+G1+NCS	T+G2+NCS	**T+I+NCS**
	25.6/32.0	24.7/28.5	27.0/30.0	26.4/30.8	25.0/28.2	24.8/28.0	24.0/28.1	**23.3/27.0**

Example 2: PDB code 2PFD, resolution 3.42Å

This structure was originally refined to R_{work} = 24.0 and R_{free} = 24.9% using a Normal Mode parameterization (Poon *et al.*, 2007). At this resolution automated water model updates were not possible.

R_{work} / R_{free} (%)	Refinement strategy							
	I	I+NCS	G1+NCS	G2+NCS	T+NCS	T+G1+NCS	T+G2+NCS	**T+I+NCS**
	21.6/28.1	20.3/26.5	21.5/28.9	22.1/29.0	21.2/27.5	21.0/27.6	21.0/28.1	**20.2/25.8**

Example 3: PDB code 1DQV, resolution 3.2Å

This structure was originally refined to R_{work} = 29.3 and R_{free} = 34.8% using the CNS program (Sutton *et al*., 1999). At this resolution automated water model updates were not possible.

R_{work} / R_{free} (%)	Refinement strategy							
	I	I+NCS	G1	G2	T	T+G1	T+G2	**T+I**
	21.6/27.9	-	25.3/30.5	24.4/29.8	22.6/27.3	21.9/26.9	21.2/27.3	**19.7/25.3**

Example 4: PDB code 1B7G, resolution 2.05Å

The PDB file header indicates R_{work} = 22.6 and R_{free} = 29.3% (Isupov et al., 1999). Winn *et al*. (2001) applied combined TLS and individual isotropic refinement which resulted in R_{work} = 22.0 and R_{free} = 25.7%.

R_{work} / R_{free} (%)	Refinement strategy						
	I	G1	G2	T	T+G1	T+G2	**T+I**
	21.4/25.2	23.1/25.8	22.9/26.4	19.7/22.5	19.1/22.5	18.9/22.0	**17.3/21.2**
	+NCS						
	21.9/25.7	22.3/26.4	23.7/26.4	20.5/22.1	20.5/22.7	19.6/21.9	17.7/21.3
	No water update, no NCS						
	20.5/26.0	22.1/26.8	22.0/27.8	19.5/24.0	18.4/22.3	19.2/24.1	16.7/21.7

Acknowledgements

This work was supported in part by the US Department of Energy under Contract No. DE-AC03-76SF00098 and NIH/NIGMS grant 1P01GM063210.

References

Afonine, P.V., Grosse-Kunstleve, R.W. & Adams, P.D. (2005). *CCP4 Newsl*. **42**, contribution 8.

Brunger, A.T. (2007). *Nature Protocols*. **2**, 2728-2733.

Chen, X., Poon, B.K., Dousis, A., Wang, Q., & Ma, J. (2007). *Structure*. **15**, 955-962.

Doyle, D.A, Cabral, J.M., Pfuetzner, R.A., Kuo, A., Gulbis, J.M., Cohen, S.L., Chait, B.T. & MacKinnon, R. (1998). *Science*. **280**, 69-77.

Dunitz, J.D. & White, D.N.J. (1973). *Acta Cryst.* A**29**, 93-94.

Isupov, M. N., Fleming, T. M., Dalby, A. R., Crowhurst, G. S., Bourne, P. C. & Littlechild, J. A. (1999). *J. Mol. Biol.* **291**, 651-660.

Ni, F., Poon, B.K., Wang, Q. & Ma, J. (2009). *Acta Cryst*. (2009). D**65**, 633-643.

Painter, J. & Merritt, E.A. (2006). *Acta Cryst*. D**62**, 439-450.

Painter, J. & Merritt, E.A. (2006). *J. Appl. Cryst*. **39**, 109-111.

Poon, B.K., Chen, X., Lu, M., Vyas, N.K., Quiocho, F.A., Wang, Q., & Ma, J. (2007). *PNAS*. **104**, 7869-7874.

Schomaker, V. & Trueblood, K.N. *Acta Cryst.* (1968). B**24**, 63-76.

Stuart, D. I. & Phillips, D.C. (1985). *Methods in Enzymology*. **115**, 117-142.

Sutton, R.B., James A. Ernst, J.A. & Brunger, A.T. (1999). *J. Cell Biol.* **147**: 589-598.

Non-periodic torsion angle targets in *PHENIX*

Jeffrey J. Headd,[a] Nigel W. Moriarty,[a] Ralf W. Grosse-Kunstleve,[a] and Paul D. Adams[a,b]
[a]*Lawrence Berkeley National Laboratory, Berkeley, CA 94720*
[b]*Department of Bioengineering, University of California at Berkeley, Berkeley, CA 94720*

Correspondence email: JJHeadd@LBL.Gov

Torsion restraints in the *PHENIX* monomer library have traditionally been parameterized with a target angle (`value_angle`), a standard deviation (`value_angle_esd`), and a periodicity (`period`) as originally specified by Vagin et al. (2004). An example mmCIF definition for the χ angles in Trp residues is shown in Fig. 1A. This periodic parameterization for χ angles proves to be insufficient to recapitulate all favored rotamer positions (Lovell et al., 2000) for Asn, Asp, His, Phe, Trp, and Tyr. For example, Fig. 2A depicts the results of geometry minimization in *PHENIX* of an ideal Tyr **m0** rotamer, which results in an **m-90** rotamer. This result occurs because the χ_2 torsion for Tyr is defined as 90° with a periodicity of 2, which excludes the 0° target. In most cases, simply increasing the periodicity of a given torsion angle is counterproductive as this will open up non-rotameric conformations in addition to the desired values.

A.

```
_chem_comp_tor.comp_id
_chem_comp_tor.id
_chem_comp_tor.atom_id_1
_chem_comp_tor.atom_id_2
_chem_comp_tor.atom_id_3
_chem_comp_tor.atom_id_4
_chem_comp_tor.value_angle
_chem_comp_tor.value_angle_esd
_chem_comp_tor.period
 TRP chi1 N  CA CB CG  180.000 15.000 3
 TRP chi2 CA CB CG CD1  90.000 20.000 2
```

B.

```
_chem_comp_tor.comp_id
_chem_comp_tor.id
_chem_comp_tor.atom_id_1
_chem_comp_tor.atom_id_2
_chem_comp_tor.atom_id_3
_chem_comp_tor.atom_id_4
_chem_comp_tor.value_angle
_chem_comp_tor.alt_value_angle
_chem_comp_tor.value_angle_esd
_chem_comp_tor.period
TRP chi1 N  CA CB CG 180.000 . 15.000 3
TRP chi2 CA CB CG CD1 90.000 0 20.000 2
```

Figure 1. Examples of the torsions section of a restraints file in CIF format for TRP.

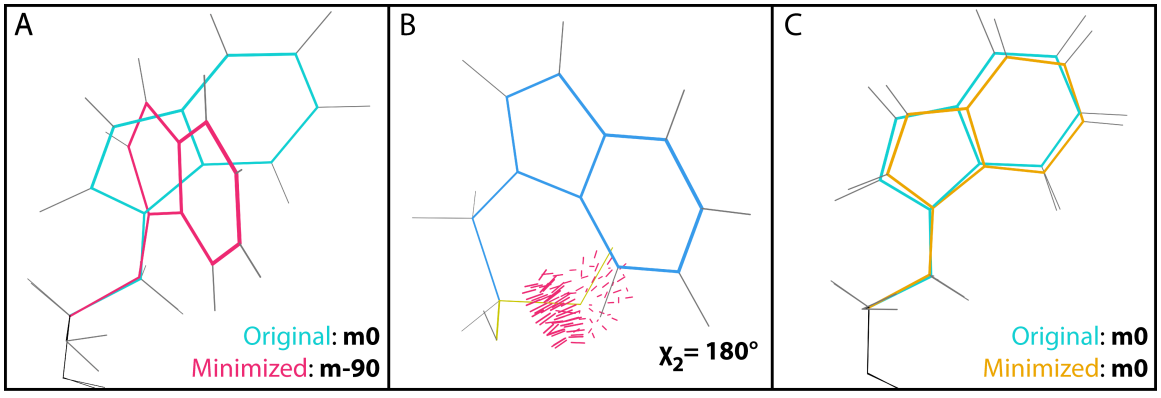

Figure 2. Geometry of various rotomers for TRP. Images generated using KiNG (Chen et al, 2009).

As shown in Fig. 2B, increasing the periodicity from 2 to 4 to allow χ_2 = 0° for Tyr opens up χ_2 = 180°, which would allow a rotamer outlier with an impossible steric clash to score favorably in the geometry term.

To recapitulate all favorable rotamer positions without introducing false-minima, PHENIX now includes an `alt_angle_value` parameter in the `tor` definitions for non-periodic parameterization of torsion angles. Fig. 1B illustrates the usage of the `alt_angle_value` parameter in the mmCIF parameterization for Tyr. This parameter takes either a single target value, or multiple target values that are comma-separated. The current `value_angle_esd` is used to apply the same ESD to the new torsion definitions as is used for the original periodic `value_angle` definition. ESD flexibility for the alternate parameter will be implemented in the future. Both `value_angle` and `alt_angle_value` may be used together for flexible implementation of torsion definitions. To allow for mixing of `tor` definitions with and withot `alt_angle_ideal` values, a '.' may be used for the `alt_angle_ideal` parameter for instances where it should be ignored by *PHENIX*.

All previously inaccessible rotamers for the above mentioned residues have been corrected in the geostd (http://geostd.sourceforge.net) in PHENIX using alt_angle_value parameters. Fig. 2C illustrates the proper recapitulation of the Tyr rotamer m0 following geometry minimization using the new parameterization. Tyr χ1 as shown in Fig. 1B demonstrates such an entry in practice.

These non-periodic torsion angle definitions may be included in any mmCIF definition for use in PHENIX, including amino acids, nucleotides, and ligands. One potential use for these parameters is for specifying sugar puckers in saccharides. Internally, eLBOW (Moriarty et al., 2009) currently uses non-periodic torsions to generate and control the puckers of saturated rings. The values of the dihedrals of a six-membered puckered ring in the chair conformer are approximately ±55 degrees. A torsion definition using periods would require a value of 60 degrees and a period of three. This is not an ideal situation for either the ideal value or the fact that 180 degrees is a minimum on the potential surface. Furthermore, the boat conformer has two torsions that are approximately zero requiring a period of six. This makes 120 degrees a possible but non-physical minimum. Testing of the non-periodic torsions for carbohydrates is currently underway and will soon be available via eLBOW.

References:

Chen, V. B., Davis, I. W. and Richardson, D. C. (2009) KiNG (Kinemage, Next Generation): A versatile interactive molecular and scientific visualization program. *Protein Science*, **18**, 2403-2409.

Lovell, S. C., Word, J. M., Richardson, J. S. and Richardson, D. C. (2000) The Penultimate Rotamer Library. *Proteins: Struct Function and Genetics*, **40**, 389-408.

Moriarty, N. W., Grosse-Kunstleve, R. W. & Adams, P. D. (2009). Acta Cryst. **D65**, 1074–1080.

Vagin, A. A., Steiner, R. A., Lebedev, A. A., Potterton, L., McNicholas, S., Long, F. and Murshudov, G. N. (2004) REFMAC5 dictionary: organization of prior chemical knowledge and guidelines for its use. *Acta Cryst.* **D60**, 2184-2195.

Model-building updates and new features

Tom Terwilliger[a]

[a]*Los Alamos National Laboratory, Los Alamos, NM 87545*

Correspondence email: terwilliger@LANL.Gov

A. Rapid phase improvement and model-building with phenix.phase_and_build (NEW)

PHENIX now has a new and very rapid method for improving the quality of your map and building a model. This `phenix.phase_and_build` approach uses all the tools described in this section. The approach is to carry out an iterative process of building a model as rapidly as possible and using this model in density modification to improve the map. This approach is related to the older `phenix.autobuild` approach. The difference is that in `phenix.autobuild` much effort was spent on building the best possible model at each stage before carrying out density modification, while in `phenix.phase_and_build` speed of model-building is optimized. The result is that `phenix.phase_and_build` is 10 times faster than `phenix.autobuild`, yet it produces nearly as good a model in the end. The `phenix.phase_and_build` approach will also find NCS from your starting map and apply it during density modification. You can run `phenix.phase_and_build` with:

```
phenix.phase_and_build my_experimental_data.mtz my_sequence.dat
```

You can also add a starting model or a starting map. This means that you can run it once, get a new model and map, then run it again to improve your model and map further.

When you run `phenix.phase_and_build` it will write out a `phase_and_build_params.eff` parameter file that can be used to re-run `phenix.phase_and_build` (just as for essentially all *PHENIX* methods). In addition, `phenix.phase_and_build` will write out the parameters files for the intermediate methods used as part of `phenix.phase_and_build` to the temporary directory used in building. You can

- Run NCS identification

  ```
  phenix.find_ncs temp_dir/find_ncs_params.eff
  ```

- Run first cycle of density modification

  ```
  phenix.autobuild temp_dir/AutoBuild_run_1_/autobuild.eff
  ```

- Run most recent model-building

  ```
  phenix.build_one_model temp_dir/build_one_model_params.eff
  ```

- Run sequence assignment and filling short gaps

  ```
  phenix.assign_sequence temp_dir/assign_sequence_params.eff
  ```

- Run loop fitting

  ```
  phenix.fit_loops temp_dir/fit_loops_params.eff
  ```

This gives you control of all the steps in map improvement and model-building in addition to letting you run them all together with `phenix.phase_and_build`.

The `phenix.autosol` wizard now uses `phenix.phase_and_build` by default for model-building. This means that now the models produced by `phenix.autosol` are quite good but are still obtained quickly.

B. Working with NCS in PHENIX with phenix.find_ncs: Identification of NCS from heavy-atom sites, from a model or from a map

The `find_ncs` method contains all the algorithms available in *PHENIX* for finding NCS, including a new algorithm for finding NCS directly from a map. The approaches used in `find_ncs` are:

1. Finding NCS from a map (NEW):

```
phenix.find_ncs my_map.mtz
```

The `find_ncs_from_density` algorithm first identifies potential locations of centers of macromolecules in the density map by finding maxima of the local RMS density. Then it cuts out a sphere of density centered at a trial center and carries out an FFT-based rotation-translation search to find all occurrences of similar density in the asymmetric unit of your map. The region over which NCS-related correlation is high is identified and the operators are written out as a "`find_ncs.ncs_spec`" file that can be read by the *PHENIX* wizards and a "`find_ncs.phenix_refine`" file that can be read by `phenix.refine`. You can run the algorithm as a whole or you can run each part separately with `phenix.guess_molecular_centers` and `phenix.find_ncs_from_density`.

2. Finding NCS from heavy-atom sites or a model

```
phenix.find_ncs ha.pdb my_map.mtz

phenix.find_ncs my_model.pdb
```

If you have a heavy-atom pdb file and a map file, then `phenix.find_ncs` will identify subsets of your heavy-atom sites that are related by non-crystallographic symmetry, and it will check whether this NCS is actually reflected in your map. It will write out the resulting NCS as `ncs_spec` and `phenix_refine` files. If you have a model with several chains that are related by NCS symmetry, `phenix.find_ncs` will find the NCS operators from the coordinates in your model.

3. Reading NCS from a my_ncs.ncs_spec file

```
phenix.find_ncs my_ncs.ncs_spec
```

will read a `ncs_spec` file written by a *PHENIX* method, and write out the NCS in formats suitable for `phenix.refine` or the wizards. If you supply also a map MTZ file, it will check for this NCS in your map.

4. Creating NCS-related copies

You can also apply NCS operators from a `my_ncs.ncs_spec` file to a single copy of your protein to create all the NCS-related copies with:

```
phenix.apply_ncs my_ncs.ncs_spec my_model_one_ncs_copy.pdb
```

C. Fitting loops with loop libraries (NEW) and by tracing chains with phenix.fit_loops

```
phenix.fit_loops my_model_with_gaps.pdb my_map.mtz my_sequence.dat
```

The `phenix.fit_loops` approach now has two main algorithms. One is to fit short gaps using a loop library derived from high-resolution structures in the PDB, and the other is to build loops directly by iterative extension with tripeptides. The loop-library approach (specified with `loop_lib=True`) is very fast, and is currently applicable for short gaps of up to 3 residues. The iterative extension approach is slower, but can be used for longer gaps (typically up to 10-15 residues).

D. Rapid building of a single model with phenix.build_one_model (NEW)

PHENIX now has a tool that you can use to quickly build a single model from a map and sequence file, or to extend an existing model. You can build a new model with resolve model-building with:

```
phenix.build_one_model my_map.mtz my_sequence.dat
```

If you supply a PDB file, then the ends of each chain in your model will be extended, if possible, based on your map.

E. Sequence assignment and short gap filling with phenix.assign_sequence (NEW)

You can now carry out an improved sequence assignment of a model that you have already built with `phenix.assign_sequence`. Further, once the sequence has been assigned, this method will use the sequence and proximity to identify chains that should be connected, and it will connect those that have the appropriate relationships using the new loop libraries available in `phenix.fit_loops`. The result is that you may be able to obtain a more complete model with more chains assigned to sequence than previously. You can run it with:

```
phenix.assign_sequence my_model.pdb my_sequence.dat my_map.mtz
```

Phenix

PHENIX website for downloads, documentation and help
www.phenix-online.org